Comparison of GC-MS, GC-MRM-MS, and GC×GC to characterise higher plant biomarkers in Tertiary oils and rock extracts

Christiane Eiserbeck [a], Robert K. Nelson [b], Kliti Grice [a,*], Joseph Curiale [a, c], Christopher M. Reddy [b]

[a] *Curtin University, WA Organic and Isotope Geochemistry Centre, Department of Chemistry, GPO Box U1987, Perth, WA 6845, Australia;* c.eiserbeck@curtin.edu.au (C. Eiserbeck)*;* k.grice@curtin.edu.au (K. Grice)

[b] *Department of Marine Chemistry and Geochemistry, Woods Hole Oceanographic Institution, Woods Hole, MA 02543, USA;* rnelson@whoi.edu (R. K. Nelson), creddy@whoi.edu (C. M. Reddy)

[c] *Chevron Energy Technology Company, 1500 Louisiana St, Houston, Texas 77002, USA* jcuriale@chevron.com (J. Curiale)

* Corresponding author. Tel.: +61 8 92663894; fax: +61 8 92663547.

Abstract

Higher plant biomarkers occur in various compound classes with an array of isomers that are challenging to separate and identify. Traditional one-dimensional (1D) gas chromatographic (GC) techniques achieved impressive results in the past, but have reached limitations in many cases. Comprehensive two-dimensional gas chromatography (GC×GC) either coupled to a flame ionization detector (GC×GC-FID) or time-of-flight mass spectrometer (GC×GC-TOFMS) is a powerful tool to overcome the challenges of 1D GC, such as the resolution of unresolved complex mixture (UCM). We studied a number of Tertiary, terrigenous oils and source rocks from the Arctic and Southeast Asia, with special focus on angiosperm biomarkers, such as oleanoids and lupanoids. Different chromatographic separation and detection techniques such as traditional 1D GC-MS, metastable reaction monitoring (GC-MRM-MS), GC×GC-FID and GC×GC-TOFMS are compared and applied to evaluate the differences and advantages in their performance for biomarker identification. The measured 22*S*/(22*S*+22*R*) homohopane ratios for all applied techniques were determined and compare exceptionally well (generally between 2-10%). Furthermore, we resolved a variety of angiosperm-derived compounds that co-eluted using 1D GC techniques, demonstrating the superior separation power of GC×GC for these biomarkers, which indicate terrigenous source input and Cretaceous or younger ages. Samples of varying thermal maturity and biodegradation

contain higher plant biomarkers from various stages of diagenesis and catagenesis, which can be directly assessed in a GCxGC chromatogram. The analysis of whole crude oils and rock extracts without loss in resolution enables the separation of unstable compounds that are prone to rearrangement (e.g. unsaturated triterpenoids such as taraxer-14-ene) when exposed to fractionation techniques like molecular sieving.

GC×GC-TOFMS is particularly valuable for the successful separation of co-eluting components having identical molecular masses and similar fragmentation patterns. Such components co-elute when analysed by 1D GC and cannot be resolved by single-ion-monitoring, which prevents accurate mass spectral assessment for identification or quantification.

1 Introduction

Comprehensive two-dimensional gas chromatography (GC×GC) is a powerful analytical tool capable of high resolution separation of complex mixtures, such as biological and geological samples (Adahchour et al., 2008; Dimandja, 2004; Eiserbeck et al., 2011; Frysinger et al., 2003; Gaines et al., 1999; Tran et al., 2010; Ventura et al., 2007). GC×GC satisfies the vision of 2D analytical separation techniques proposed 25 years ago by Giddings (1984). The resolution power of GC×GC is based on the combination of two GC columns with different, orthogonal stationary phases, e.g. non-polar (100% dimethylpolysiloxane) and polar (50% phenyl-, 50% dimethylpolysiloxane).

The enhanced peak capacity allows for simultaneous analysis of saturated and aromatic compounds, and mapping of chemical classes in distinct pattern within the chromatogram (e.g. Ventura et al., 2010).

The vastly expanding peak resolving capacity of GC×GC makes it an ideal choice for analysis of complex mixtures such as crude oil, source rock extracts, or refined products (Adahchour et al., 2008; Adahchour et al., 2006; Aguiar et al., 2010; Frysinger and Gaines, 2001; Li et al., 2008; Silva et al., 2011; Tran et al., 2006; Tran et al., 2010; Ventura et al., 2011; Ventura et al., 2008; Ventura et al., 2010; Wang and Walters, 2007). GC×GC is particularly well suited to monitor changes in biomarker distributions over time, for instance during gradual biodegradation of spilled oil in the

environment (Nelson et al., 2006) or the identification of their sources (Gaines et al., 2006; Lemkau et al., 2010). Previous reports focus mainly on crude oil fingerprinting (Ventura et al., 2011; Ventura et al., 2010), and characterisation of unresolved complex mixture (UCM) in biodegraded oils (Frysinger et al., 2003; Tran et al., 2010; Ventura et al., 2008). All of these studies focussed on hopanoids and steroids as well as common aromatic biomarkers such as naphthalenes and phenanthrenes (e.g. Aguiar et al., 2010; Silva et al., 2011). However, the application of GC×GC to plant biomarkers has not been thoroughly investigated to date. Separation of 18α(H)- and 18ß(H)-oleanane (**I** and **II**) and lupane (**III**) in Tertiary oils was described in detail by Eiserbeck et al. (2011) and Silva et al. (2011). Angiosperm biomarkers, such as oleanoids and lupanoids, are relevant indicators for terrigenous origin and are important age-diagnostic biomarkers as they indicate Cretaceous or younger aged source rocks (Ekweozor and Udo, 1988; Moldowan et al., 1994).

Various isomers have been identified among the diagenetic products of saturated, unsaturated, and aromatic pentacyclic and tetracyclic (ring A-degraded) oleanoids, ursanoids and lupanoids. However, many more are likely to co-exist as stereoisomeric mixtures. Such mixtures are very challenging to separate chromatographically due to their nearly identical structures, which result in very similar elution properties. 18α(H)- and 18ß(H)-oleanane (**I** and **II**), for example, co-elute on typical non-polar columns (1D GC-MS; Nytoft et al., 2002) and have similar mass spectra,

96 thus preventing separation based on mass spectral characteristics. GC×GC
97 was proven to effectively resolve stereoisomers of hopanes and steranes
98 (Frysinger and Gaines, 2001; Silva et al., 2011) and thus appears to be the
99 preferred choice to study minor components in complex mixtures of isomeric
100 plant biomarkers.
101 This study applies GC×GC-FID and GC×GC-TOFMS to analyse a set of
102 Tertiary oils and rock extracts with various plant biomarker contents. The
103 samples also differ in their relative thermal maturity and degree of
104 biodegradation. This allows identification of plant markers in the
105 consecutive stages of catagenesis and investigation of the resolution power
106 for low abundance biomarkers in highly biodegraded oils. A GC×GC method
107 was developed that allows easy access to common geochemical parameters
108 and information without sacrificing the best possible separation of specific
109 plant biomarkers. The GC×GC separation results are compared with
110 traditional 1D GC separations focussing on 2D resolution of 1D co-elution
111 problems.

2 Experimental

2.1 Samples

Two sets of Tertiary samples were included in this study: nine oils (Table 1) and 10 rocks (Table 2). The samples were grouped according to their origin from the Arctic (Canadian Beaufort-Mackenzie Delta and Alaskan North Slope) or Southeast Asia (Myanmar, Brunei, Indonesia; see Table 1). One additional marine oil from California was included in the set for comparison. The source ages of all oil samples were determined prior to this study by oil – source rock correlation and basin modelling studies. The samples show signs of varying degrees of maturity, mixing, migration contamination, and biodegradation (Peters et al., 2005b), which allows comparison of the assessment of these processes using the different analytical techniques. Rock samples were ground and Soxhlet extracted for 72 hours using dichloromethane (DCM). The crude oil samples and rock extracts were fractionated by liquid chromatography as described in Maslen et al. (2009). The saturated hydrocarbons were further separated into *n*-alkanes and branched and cyclic hydrocarbons by 5A molecular sieving (Dawson et al., 2005; Grice et al., 2008). Standards for the following compounds were purchased from Chiron and were co-injected for identification in all three techniques: 18α(H)- and 18ß(H)-oleanane, lupane, 18ß(H)-olean-12-ene, lup-22(29)-ene, 17α- and 17ß(H)-28-norlupane, 28-norlup-16(17)-ene, 28-norlup-

17(22)-ene, urs-12(13)-ene. The standard for 24,28-bisnorlupane was extracted from the Maraat oil. Further compounds were tentatively identified *via* retention time and mass spectral comparison with the literature.

2.2 Gas chromatography – mass spectrometry (GC-MS)

GC-MS analyses were performed using a Hewlett Packard (HP) 6890 gas chromatograph interfaced with a HP 5973 mass spectrometer. The GC was fitted with a 60 m x 0.25 mm i.d. WCOT fused silica capillary column coated with a 0.25 μm thick film of 5% phenyl-, 95% dimethylpolysiloxane (DB-5). Ultra high purity He was used as carrier gas with a constant flow rate of 1 mL min^{-1}. Samples were dissolved in *n*-hexane and injected at 310 °C in splitless mode (split vent opened after 0.5 min) using a HP 6890 series autosampler. The GC oven was programmed from 40 °C to 310 °C at 3 °C min^{-1} with initial and final hold times of 1 and 30 min, respectively. All fractions were analysed in full scan (50 – 550 amu) and in single ion monitoring (SIM) mode (Appendix 4).

Areas for the calculation of biomarker ratios were determined from SIM analyses using the base ions for each peak unless otherwise noted.

2.3 Gas chromatography – metastable reaction monitoring - mass spectrometry (GC-MRM-MS)

Metastable reaction monitoring (MRM) analysis of the branched/cyclic hydrocarbons was performed using a Fisons Autospec Ultima Q hybrid MS-MS operated in MRM mode. The HP 5890 Series II gas chromatograph was fitted with a cool on-column injector and a HP 7673 autosampler. The same capillary column as in the GC-MS experiments was used. Samples in *n*-hexane were injected at 50 °C with a hold time of 1 minute. The oven was then heated at 3 °C min^{-1} to 310 °C and held at that temperature for 20 minutes. The resolution was set at 500 with a dwell time of 20 ms, 8000 V accelerating voltage and a source temperature of 200 °C. All saturated fractions were analysed in full scan mode (40-540 amu) and in metastable reaction monitoring (MRM) mode (Appendix 4). A set of mass spectrometer methods was used, each tailored to monitor different parent/daughter ion transitions corresponding to tricyclic, tetracyclic and pentacyclic terpanes (Appendix 3). Data acquisition started at 40 minutes.

Peak areas for the calculation of biomarker ratios were determined using the most abundant transition, generally the transition of the molecular ion (M^+) to the base ion. In the case of co-elution in this transition, the next abundant transition without co-elution was used consistently for all samples to assure comparability.

2.4 Comprehensive two-dimensional gas chromatography (GC×GC)

For GC×GC analysis, whole crude oil samples and rock extracts were dissolved in a solution of 5% DCM in *n*-hexane and asphaltenes were decanted.

Two Leco Pegasus 4D GC×GC systems were used in this study coupled with a TOFMS and a FID, respectively. They were equipped with an Agilent 6890N GC (TOFMS) and an Agilent 7890 GC (FID system) and configured with a split/splitless auto-injector (7683B series) and a dual stage cryogenic modulator (Leco, Saint Joseph, Michigan). The modulator operates with a cold and hot jet. The cold jet gas was dry N_2, chilled with liquid N_2. The hot jet was operated with air that was heated at 55 °C above the temperature of the main GC oven. Two capillary GC columns were fitted in the GC. The first-dimension column was a 100% - dimethylpolysiloxane coated column (Restek Rtx-1MS Crossbond, 25 m length (TOF)/ 20 m (FID), 0.20 mm I.D., 0.2 µm film thickness), whereas the second-dimension separations were performed on a 50% phenyl polysilphenylene-siloxane column (SGE BPX50, 1.25 m length (TOF)/1 m (FID), 0.10 mm I.D., 0.1 µm film thickness).

For GC×GC-TOFMS analysis, 3 µL of a 50 mg mL^{-1} solution were injected into a 300 °C splitless injector with a purge time of 0.5 min. For GC×GC-FID analysis, 1 µL of a 4.5 mg mL^{-1} solution was injected under the same conditions. The first-dimension column and the dual stage cryogenic

modulator reside in the main oven, whereas the second-dimension column is fitted in a separate oven, allowing for independent temperature control. Helium (hydrogen for the FID system) was used as carrier gas at a constant flow rate of 1.05 mL min^{-1} (0.95 mL min^{-1} for the FID system).

The temperature program for the main oven started isothermal at 45 °C (10 min) and was then ramped from 45 to 317 °C at 1.25 °C min^{-1}. The hot jet was pulsed for 0.75 second every 10 seconds with a 4.25 second cooling period between stages. A modulation period of 10 seconds was chosen in order to avoid "wrapping". Although a shorter modulation period allows for better first dimension separation, polar compounds, e.g. with four to six aromatic rings, might not elute from the second dimension column within the modulation period, resulting in "wrapping" and subsequent misrepresentation of their first and second dimension retention times. The second dimension oven was programmed from 68 °C (10 min) to 340 °C at 1.25 °C min^{-1}.

The TOFMS data were sampled at an acquisition rate of 50 spectra per second. The transfer line from the second oven to the TOFMS was deactivated fused silica (0.5 m length, 0.18 mm I.D.), constantly held at 280 °C. The TOF detector voltage was 1525 Volts and the source temperature was 225 °C. The mass spectrometer employs 70 eV electron ionisation and operates at a push pulse rate of 5 kHz. This allows sufficient signal averaging time to ensure good signal-to-noise ratios while still operating at a sufficient data acquisition rate to accurately process (signal

217 average) spectra for peaks eluting from the second dimension column with
218 second dimension peak widths on the order of 50 to 200 milliseconds. The
219 FID signal was sampled at 100 Hz.

3 Results and Discussion

3.1 GC-MS and GC-MRM-MS analysis

All of the samples were initially analysed using 1D GC-MS and GC-MRM-MS. These analyses were used to screen the oils and extracts for a rapid assessment of biomarker composition and general characteristics. GC–MS chromatograms of the saturated fractions are shown in Fig. 1. All samples (except CA) have substantial input of land plant biomarkers.

3.1.1 Arctic oils

The non-biodegraded oils A1 and C4 show geochemical characteristics typical of land-plant derived organic matter, such as high pristane (Pr) to phytane (Ph) ratios (Table 1), abundant tri- and tetracyclic diterpanes (Noble et al., 1985), and a strong predominance of the C_{29} steranes compared to their C_{27} and C_{28} homologues (Table 1; Philp and Gilbert, 1986). Although oil C2 has only reached biodegradation rank 1 (Table 1), the saturated trace shows a pronounced UCM (Figure 1). Furthermore, the C_{32} 22*S*/(22*S*+22*R*) hopane ratio is only 0.53, although the endpoint for this homolog is generally assumed to be 0.58 for early-mature oil (Zumberge, 1987). The C_{29} 20*S*/(20*S*+20*R*) and the C_{29} ββ/(αα+ββ) sterane ratios both are low (0.14 and 0.36, respectively). The relatively high UCM for this otherwise

239 early-mature oil with only slightly degraded *n*-alkanes suggests that C2 is
240 possibly a mixture.
241 C2 has an odd-even-predominance (OEP, n-C_{25} - n-C_{29}) value of 1.5. The
242 OEP is most pronounced in immature organic matter and diminishes with
243 increasing thermal maturity. Thus, the absence of OEP in most oils despite
244 the significant land plant input can be explained by elevated thermal
245 maturity. C2 is most likely mixed with immature organic matter that still
246 contains the indigenous OEP.
247 The oils A2, A3, and C3 have significant plant biomarker input. However,
248 many of these biomarkers cannot be assessed since these oils were subject to
249 heavy or severe biodegradation (Table 1), which altered or removed the
250 indicative biomarkers such as Pr, Ph, or steranes. A2 and A3 experienced
251 complete loss of *n*-alkanes, isoprenoids, trimethylnaphthalenes and all
252 regular steranes. The homohopanes C_{32} – C_{35} are partially degraded.
253 Interestingly, these compounds are still present at a biodegradation rank 7
254 with all regular steranes removed. A series of 25-norhopanes was identified
255 ranging from C_{27} (25,28,30 – trisnorhopane, I) up to C_{33}. Occurrence of these
256 hopanoids supports the high degree of biodegradation in oils A2 and A3
257 (Bennett et al., 2006; Peters et al., 1996; Volkman et al., 1983). The relative
258 amount of UCM is substantial and complicates the GC analysis, separation,
259 and identification using traditional 1D techniques.

Oil C3 shows signs of moderate to heavy biodegradation with the loss of most of the *n*-alkanes and isoprenoids and partly degraded methylnaphthalenes.

3.1.2 Southeast Asian oils

No odd-over-even predominance was observed in oils M1 and M2 from Myanmar. However, abundant angiosperm biomarkers and the highest Pr to Ph ratios amongst the oils (4.8 and 5.3, respectively; Table 1) indicate strong land plant input to the source organic matter. Specific to the oils from Myanmar is the presence of bicadinanes (**IV**). Bicadinanes (**IV**) are mainly derived from dammar resins of the extant angiosperm family *Dipterocarpaceae* (van Aarssen et al., 1990a; van Aarssen et al., 1994), that first occurred in Southeast Asia in the Oligocene (Morley, 2000). The age and location of the two oils from Myanmar agree with this observation. Bicadinanes (**IV**) were not found in the Arctic oils, which are younger and originated in a cooler climate. Bicadinanes (**IV**) have been reported to be sourced from other resinous angiosperms outside the palaeogeographical range of the dipterocarps such as fossil fruit from an ancient representative of mastixioid *Cornaceae,* which occurred in the Messel Shale, deposited under cooler climate conditions. However, these observations are rare and the main source for bicadinanes (**IV**) remains the dammar resin (Crelling et al., 1991; Murray et al., 1994; van Aarssen et al., 1994).

3.1.3 Californian oil

The Californian condensate CA is from a marine source rock and was included for comparison with the terrigenous sourced oils. Its molecular composition is dominated by *n*-alkanes and isoprenoids. Abundant *n*-C_{16} – *n*-C_{19} (Gelpi et al., 1970; Grice et al., 1997; Tissot and Welte, 1984), the absence of terrigenous biomarkers, and the lack of OEP in the range of *n*-C_{27} – *n*-C_{35} (Eglinton and Hamilton, 1967) support a marine source for this condensate. The concentrations of the hopanoids and steranes are below 10 ppm.

3.1.4 Arctic rock samples

The Arctic rock samples generally show an *n*-alkane distribution maximising around *n*-C_{17}. Their Pr/Ph ratios range between 0.8 and 1.9 (Table 2) and only a subtle odd-even predominance between *n*-C_{25} – *n*-C_{29} is observed (1.2 – 2.2). Sample S1 is an exception, with immature biomarker signals such as the presence of the 17ß,21ß(H)-hopanoid series and a very dominant 22*R*-C_{31} - homohopane over the 22*S*-isomer. In contrast, the C_{32} – C_{35} homohopanes show a more mature signal for the 22S/22R isomerisation ratio, suggesting possible migration contamination.

The terrigenous signatures in the Arctic rock extracts are mainly attributed to relatively abundant oleanoids (Moldowan et al., 1994; Nytoft et al., 2002), lupanoids, isopimarane (**V**), abietane (**VI**) or simonellite (**VII**) (Otto and Wilde, 2001). Extract S1 is the oldest sample in the set (Late Paleocene,

303 Table 2) and is dominated by conifer biomarkers like isopimarane (**V**),
304 norisopimarane (**VIII**), cadalene (**IX**) and simonellite (**VII**) as opposed to
305 angiosperm biomarkers, which is consistent with its age. Angiosperms
306 evolved in the Cretaceous or earlier, but only became prominent during the
307 Tertiary (Moldowan et al., 1994).

308 *3.1.5 Rocks from Southeast Asia*

309 Two rocks from Brunei and one coal from Indonesia included in the sample
310 set contain substantial land plant signals. Extract S9 and S10 (Table 2)
311 have exceptionally high concentrations of unsaturated angiosperm derived
312 pentacyclic triterpenoids (200 - 1100 ppm compared to 1 - 50 ppm in the
313 oils). S9 has a strong predominance of C_{29} steranes (87%, Table 2) and an
314 OEP of 2.3, while the Pr/Ph ratio is 0.83. Extract S10 has the highest Pr/Ph
315 ratio (6.1) and a strong contribution of bicyclic land plant markers, such as
316 cadinane (**X**) and eudesmane (**XI**) (Alexander et al., 1984; Noble et al., 1986).
317 The rock extracts from Brunei show relatively low thermal maturity based
318 on the low sterane and hopane isomerisation ratios (Table 2). Extract S10
319 shows conflicting maturity parameters. Regular steranes occur only in their
320 biological ααα*R* configuration (Mackenzie et al., 1982), which is unstable
321 during burial, while abundant aromatised plant markers – 1,2,9- and 2,2,9-
322 trimethyl-1,2,3,4-tetrahydropicene (**XII** and **XIII**) (Freeman et al., 1994) or
323 tetranor-oleanana(ursa)heptaene (**XIV**) (Jacob et al., 2007) - suggest higher
324 thermal maturity. Aromatisation occurs much later during catagenesis or as

325 a parallel pathway to ring-opening or partial degradation during diagenesis
326 controlled by the depositional conditions (Rullkötter et al., 1994; Stout,
327 1992). The concurrent presence of both abundant mono- and di-unsaturated
328 triterpenoids and their tetraaromatic equivalents suggests contamination by
329 a relatively more mature crude oil that is similarly rich in land plant
330 biomarkers.
331 The most peculiar extract is S8, as it consists of mainly one peak, an
332 unidentified tetracyclic triterpenoid (Fig. 1k). An OEP ratio of 8.7 supports a
333 terrigenous origin. The low abundance of *n*-alkanes, and absence of
334 isoprenoids are more likely a source effect, because no UCM was observed.

335 **3.2 GC×GC-TOFMS and GC×GC-FID analysis**

336 In the GC×GC chromatograms, compound classes are separated across the
337 2D plane spanned by the first and second dimension (Fig. 2; Ventura et al.,
338 2010) according to their increasing volatility (non-polar column, first
339 dimension) and polarity (polar column, second dimension). Aromatic
340 compounds elute further in the polar dimension than saturated compounds,
341 and thus can be distinguished easily in whole oil analysis. Most abundant
342 compounds/compound classes, main features, and general similarities
343 between oils, such as A2 and A3 (Fig. 2 b, c), appear clearly in much more
344 detail than possible using traditional 1D GC analysis.
345 Reliable identification of biomarkers is achieved based on the first and
346 second dimension retention times (^1t_R and ^2t_R) and the biomarker

fingerprint within the distinct elution pattern of the compound classes. Once these are established e.g. by analysis of standards, volumes are best determined using FID. The advantage of GC×GC-FID compared to the TOFMS is the quantitative detection of peak abundances, reproducibility, increased sensitivity (~5 times), and improved peak shape (Eiserbeck et al., 2011). In comparison, GC×GC-TOFMS and GC×GC-FID complement each other and the use of both systems is recommended. Similar response factors for all hydrocarbons in a GC×GC-FID chromatogram improve the comparability of obtained concentrations. The retention time stability for multiple GC×GC-FID analyses of 17α,21ß(H)-hopane measured in standard deviation of the RT compared to the TOFMS was 5 s and 0.014 s for $^{1}t_{R}$ and $^{2}t_{R}$ compared to 17 s and 0.066 s for TOFMS.

3.3 Comparison GC-MS, GC-MRM-MS, GC×GC-TOFMS, GC×GC-FID

In order to compare traditional 1D GC techniques with the results obtained by GC×GC multiple GC-MS methods (full scan and SIM) and GC-MRM-MS methods, tailored to each compound class, had to be applied to identify all biomarkers of interest, namely hopanoids, steranes, ring A-degraded, saturated, unsaturated, and aromatic pentacyclic triterpenoids (Appendix 4). The results of these numerous analyses per sample were compared to GC×GC analysis based on only one method applied to the whole crude oil or

368 rock extract without prior liquid chromatographic fractionation, which can
369 introduce contamination or cause loss of volatile compounds.

370 *3.3.1 Biodegradation*

371 Fig. 4 illustrates the improvement in separation of the severely biodegraded
372 oil A2. The GC-MS chromatogram (SIM analysis, 17 ions, Appendix 2) of the
373 saturated hydrocarbon fraction of oil A2 shows a prominent UCM, which is
374 reduced compared to the full scan chromatogram (Fig. 1b). This is expected
375 because fewer ions are monitored in SIM compared to full scan.
376 Nonetheless, the UCM still adds significant noise to the mass spectra and
377 alters the baseline of the SIM chromatogram. GC-MRM-MS reduced the rise
378 in the baseline caused by the UCM to near zero (Fig. 4b). On the downside,
379 GC-MRM-MS relies on only one or two transitions per compound for
380 identification, which increases the sensitivity but prevents positive
381 identification of many biomarkers based on their mass spectra. The second
382 dimension separation in GC×GC-TOFMS resolves most of the compounds
383 from the UCM (Fig. 4c), while retaining full mass spectral information for
384 identification.

385 *3.3.2 Maturity*

386 Silva et al. (2011) demonstrated the use of thermal maturity parameters
387 from GC×GC-TOFMS. But how do these parameters compare to data
388 obtained from 1D GC techniques? Evaluation of the isomerisation ratio

389 $S/(S+R)$ of C_{32} homohopanes, one of the most commonly applied thermal
390 maturity parameters (Table 1, Table 2; Peters et al., 2005b), obtained from
391 GC-MS, GC-MRM-MS, GC×GC-FID and GC×GC-TOFMS proves GC×GC
392 data to be comparable with the more traditional techniques (Fig. 5,
393 Appendix 3).
394 This is important for the application of GC×GC to screen oils and rocks,
395 acquire much better resolved molecular data and maintain comparability to
396 biomarker data reported in the past based on 1D analysis. Generally, at
397 least three of the four determined ratios per sample are in exceptional
398 agreement, mostly within analytical error (≤ 5%, Appendix 3). The rather
399 low value of 0.43 measured for oil A3 is an artefact of biodegradation. The
400 $22S/(22S+22R)$ values for both severely biodegraded oils A2 and A3 are
401 unreliable. Nevertheless, the ratios obtained from all four techniques are in
402 very good agreement for these oils.
403 Oil CA, along with rock extracts S9 and S10, show the largest range of
404 $22S/(22S+22R)$ values among the oils due to the very low abundance of
405 homohopanes, challenging the detection limits of each system. This is a
406 general trend in the data set: lower abundance corresponds to a wider range
407 of $22S/(22S+22R)$ values determined using the different techniques. The
408 impact of analytical error increases with decreasing peak size. Altogether,
409 the ratios for S10 obtained from GC×GC-FID and GC×GC-TOFMS compare
410 very well in contrast to the 1D GC values, suggesting more reliable results
411 from the GC×GC applications.

3.4 Hopanes

Naturally occurring 17ß,21ß(H)-hopanes and the series of altered epimers, such as C_{27} – C_{35} 17ß,21α(H)-moretanes, 17α,21ß(H)-hopanes, 25-norhopanes are separated by GC×GC not only in the first dimension, as in traditional 1D GC, but also in the second dimension (Fig. 6, see also Aguiar et al., 2010), resolving co-elution of hopanes with very similar mass spectra. 25-Norhopanes elute relatively early in ^2t_R, well before regular α,ß-hopanes followed by the ß,α-hopanes (moretanes). The longest ^2t_R were observed for the ß,ß-hopanes, which elute considerably later in the second dimension. All series create a distinct, recognisable pattern in the chromatogram (Fig. 6). An uneven, non-Gaussian peak shape was observed for C_{30} 17α,21ß(H)-hopane in a number of samples in this study, but was also observed in the GC×GC-TOF chromatogram of a terrigenous oil from Brazil (Fig. 1c; Silva et al., 2011). Closer investigation of the high resolution GC×GC-TOFMS chromatogram revealed at least four partially co-eluting compounds, all of which contain *m/z* 177 and *m/z* 191 mass fragments, contributing to the extracted ion chromatograms commonly used to quantify C_{30} hopane. These compounds are relatively abundant in samples S5 and S6 and thus were visually recognisable. However, they are also present in minor concentrations in the Canadian oils C2 –C4 and the Alaskan oils, affecting quantification results using the *m/z* 191 ion trace. Compounds 1 to 3 (Fig. 7) have a molecular mass of M^+ 398 indicative of a C_{29} triterpenoid. Characteristic mass spectral features of compound 1 are the equally

435 abundant *m/z* 177 and *m/z* 191 fragments, similar to 30-normoretane,
436 which elutes later in the first dimension, between C_{30}-hopane and C_{31}-
437 homohopane. Compound 2 elutes next to compound 1 and shows an
438 intensive *m/z* 177 fragment ion and an unusual *m/z* 255 fragment ion.
439 Compound 3 elutes next to C_{30}-hopane. It has an intense *m/z* 191 ion and a
440 relatively abundant *m/z* 355 ion representing the loss of an isopropyl group
441 [M^+ 398 – 43]. Isopropyl groups are present in the structures of hopanoids,
442 lupanoids and ring A-contracted oleanoids (Smith, 1995). The relatively
443 abundant *m/z* 355 ion suggests a norlupane or demethylated *abeo*-oleanane
444 isomer. Peaks 4a and 4b (Fig. 7) appear to be two different peaks, but they
445 have nearly identical mass spectra and therefore are both attributed to
446 hopane, eluting in two consecutive modulation periods. Peaks with first
447 dimension peak widths (generally about 20-25 seconds) longer than the
448 modulation period – commonly 4 - 10 s - are split and elute in two (or more)
449 slices. This can cause slight retention time shifts and the appearance of two
450 peaks, depending on the distribution of the peak between the two slices.
451 Compounds 1 to 3 may interfere when quantifying C_{30} hopane using the
452 *m/z* 191 ion trace.

453 **3.5 Steranes**

454 Under the applied GC×GC conditions in this study, all common steranes are
455 well separated in the first and second dimension (Fig. 6). Diasteranes elute
456 earlier in the second dimension (non-polar/polar column configuration) and

457 are well separated from the regular steranes. Furthermore, the 1D GC co-
458 elutions of steranes and bicadinanes (**IV**) were resolved by GC×GC. The
459 characteristic mass fragment ion for steranes (*m/z* 217) is also present in
460 bicadinanes (**IV**). As a consequence, GC-MRM-MS analysis was required so
461 far for reliable quantification of these two biomarker groups. Applying
462 GC×GC, bicadinanes (**IV**) elute earlier in the second dimension compared to
463 steranes. This is particularly interesting as bicadinanes (**IV**) are reported as
464 pentacyclic compounds (van Aarssen et al., 1990b) and are therefore
465 expected to elute later in the second dimension along with other pentacyclic
466 compounds. Compound classes, such as tetracyclic or pentacyclic saturated
467 compounds, elute in characteristic areas of the two-dimensional
468 chromatographic plane, which forms a pattern based on the volatility (first
469 dimension) and polarity (second dimension) associated with the relevant
470 core structure (e.g. Fig. 2, 3). The early elution of bicadinanes (**IV**) suggests
471 a tetracyclic structure, contradicting the existing structural model.
472 Anderson and Muntean (2000) came to a similar conclusion based on NMR
473 analysis of dammar resin, inviting re-evaluation of the proposed structure.

474 **3.6 Plant markers**

475 *3.6.1 Des-A-triterpenoids*

476 A number of angiosperm des-A-triterpenoids were detected in all of the
477 terrigenous samples. Des-A-oleanane (**XV**) and des-A-lupane (**XVI**) are ring

A-degraded triterpenoids that were reported along with des-A-ursane (**XVII**), des-A-taraxastane (**XVII**), and C_{24}-17,21-secohopane (des-E-H, **XVIII**) as the most abundant tetracyclic triterpenoids in oils and rocks from the Taranaki Basin (Sandison, 2001; Woolhouse et al., 1992) and the Niger Delta (Samuel et al., 2010). However, des-A-ursane (**XVII**) and des-A-taraxastane (**XVII**) appear to be attributed to the same peak (e.g. Sandison, 2001; Woolhouse et al., 1992). These compounds are diastereomers. Confusion about taraxastane and ursane has been noted previously (ten Haven et al., 1993; Zhou et al., 2003). Reports in the literature are inconsistent when applying the names ursane or taraxastane or unspecific as to which stereochemistry applies. Perkins et al. (1995) distinguished 19α(H)-taraxastane (**XIX**) from ursane (**XX**) based on the stereochemistry of the hydrogen at C_{18} (Ames et al., 1954), equivalent to 18α(H)- and 18β(H)-oleanane (**I** and **II**). Other reports differentiate taraxastane (**XXI**) and ursane (**XX**) by the stereochemistry of the methyl groups at C_{19} and C_{20} (Sandison, 2001). While the C_{30} compound eluting just before 22*S*-C_{31}-homohopane (on regular non-polar columns) was proposed to be taraxastane (**XXI**) rather than ursane (**XX)**, the C_{24} des-A-compound eluting between des-A-L (**XVI**) and des-E-H (**XVIII**) is often identified as des-A-ursane (**XVII**) based on elution order. However, the exact stereochemistry of this compound has yet to be determined. In the following this compound is referred to as des-A-U/T (**XVII**).

Des-A-Ol (**XV**), des-A-L (**XVI**) and des-E-H (**XVIII**) were positively identified in all terrigenous oils in this study based on comparison with the literature (Huang et al., 2008; Huang et al., 1995; Jacob et al., 2007; Logan and Eglinton, 1994; Stefanova et al., 2008; Woolhouse et al., 1992). However, the identification of peak 1 (Fig. 8a) was conflicting. The relative retention time of this peak supported des-A-U/T (**XVII**), whereas mass spectral comparison with data presented by Woolhouse et al. (1992) was not satisfactory. Peak 1 has equally abundant mass fragments *m/z* 177 and *m/z* 191 (Fig. 8c) which was not observed by Woolhouse et al. (1992). Therefore, GC×GC analysis was used for further confirmation. In GC×GC chromatograms, the four generally most abundant tetracyclic triterpenoids are not only separated in the first, but also in the second dimension and elute in a distinct pattern (Fig. 8a, b). The $^{2}t_{R}$ offset between des-A-oleanane (**XV**) and peak 1 is similar to the offset between their pentacyclic homologues oleanane (**I**) and taraxastane (**XXI**), further supporting peak 1 to be des-A-U/T (**XVII**). An oil from the Niger Delta and three oils from the Taranaki Basin (Maui-1, McKee and Kora wells) were analysed by GC×GC-TOFMS under the same conditions. Reports on these oils included only des-A-Ol (**XV**), des-A-L (**XVI**), des-A-U/T (**XVII**), and des-E-H (**XVIII**) as ring A-degraded triterpenoids (Sandison, 2001; Woolhouse et al., 1992). After comparison of retention times and mass spectra for these oils and the samples in this study, peak 1 was positively identified as des-A-U/T (**XVII**). The marine condensate CA lacks any angiosperm derived triterpenoids, as expected for a marine oil

523 with little to no higher plant input. Elevated concentrations in the Arctic
524 oils C2 and C3 and with normal concentrations for C4 and other oils and
525 extracts from the Arctic and Southeast Asia suggest that the abundance of
526 des-A-compounds is not controlled by changes in plant communities with
527 latitude, supporting a common plant source. Coal S8 is an exceptional
528 sample that contains almost exclusively tetracyclic triterpenoids. Des-A-L
529 (**XVI**) and des-E-H (**XVIII**) are very abundant whereas des-A-Ol (**XV**) and
530 des-A-U/T (**XVII**) are absent. However, the by far most abundant compound
531 in this coal is the unidentified ring A-degraded compound 5, which elutes
532 just after des-A-U/T (**XVII**) (Fig. 8b). A second unidentified compound 6
533 elutes between compound 5 and des-E-H (**XVIII**). Apart from S8, compound
534 5 is the most abundant des-A-compound in rock extracts S1, S2, S5, S7 and
535 S10. S8 and S9 contain compound 5 in minor concentrations. It is absent in
536 S3, S6, and all oils. Compound 6 was only observed in S8. Although absent
537 in all of the oils, compound 5 is probably not a contaminant because the
538 fragmentation pattern in the mass spectrum has strong triterpenoid
539 characteristics. The similar mass spectral characteristics of compounds 5
540 and 6 (Fig. 8e, f) compare well to those of des-A-oleanane (**XV**) with a
541 relatively abundant m/z 206 mass fragment in compound 5. A similar
542 compound was described by Jacob et al. (2007) in lake sediments, although
543 it was attributed to des-A-oleanane/ursane (**XVII**).
544 Furthermore, GC×GC-TOFMS analysis improved the separation of the
545 series of saturated C_{24} des-A- and nor-des-A-compounds and their mono-

546 and di-unsaturated homologues in the first and second GC×GC dimension.
547 All of these series show similar elution patterns and elute parallel to each
548 other shifted in $^{1}t_R$ and $^{2}t_R$. Des-A-lupane (**XVI**) and a nor-des-A-compound
549 tentatively identified as nor-des-A-U/T (**XVII**) co-elute in the first
550 dimension, but were resolved in the second dimension (Fig. 9a). Similar
551 separation results were achieved for the mono- and di-unsaturated des-A-
552 series (M^+ 328, M^+ 326) (Fig. 9b). Des-A-lupene and des-A-lupadiene
553 (tentatively identified *via* mass spectral analysis, loss of isopropyl group
554 [M^+-43]) are resolved from compounds 7 (M^+ 328) and 8 (M^+ 326),
555 respectively.
556 These separations are of particular value as each pair of mono- and di-
557 unsaturated compounds co-eluting in first dimension has identical
558 molecular masses. In traditional 1D GC, complete co-elution in combination
559 with the same molecular masses prevents identification of individual mass
560 spectra and therefore identification and quantification of either compound.
561 GC×GC analysis of whole oils facilitates identification of diagenetically
562 related products. Saturated, mono-, di-, and triaromatic tetracyclic
563 triterpenoids can easily be determined with the help of the two retention
564 times. Increasing $^{2}t_R$ responds to increasing polarity, i.e. aromaticity; mono-,
565 di-, and triaromatic compounds elute along a line within the 2D
566 chromatogram plane (Fig. 9c).
567 Very good separation in the second dimension was achieved for
568 monoaromatic des-A-compounds (M^+ = 310) and triaromatic pentacyclic

569 triterpenoids (M^+ = 342), which were found to co-elute in GC-MS
570 chromatograms.

571 *3.6.2 Pentacyclic triterpenoids*

572 GC×GC separation of angiosperm derived, saturated pentacyclic
573 triterpenoids 18α(H)-, 18ß(H)-oleanane (**I** and **II**) and lupane (**III**) was
574 reported by Eiserbeck et al. (2011). The resolution of 18α(H)-oleanane (**I**)
575 and lupane (**III**) using a similar column combination was reported by Silva
576 et al. (2011). Interestingly, they achieved the opposite elution order for
577 18α(H)-oleanane (**I**) and lupane (**III**) compared to Eiserbeck et al. (2011).
578 Silva et al. (2011) found lupane (**III**) to elute earlier in both the first and
579 second dimension, while Eiserbeck et al. (2011) reported a longer retention
580 time in both dimensions for lupane (**III**) compared to 18α(H)-oleanane (**I**).
581 Furthermore, Silva et al. (2011) did not report the elution order of 18ß(H)-
582 oleanane (**II**) relative to the 18α(H)-isomer (**I**) and lupane (**III**). 18α(H)-
583 oleanane (**I**) is the thermally more stable isomer and forms by isomerisation
584 of the biologically occurring but thermally less stable 18ß(H)-oleanane (**II**)
585 up to an equilibrium ratio (Riva et al., 1988). Thus, 18α(H)-oleanane (**I**)
586 without coexisting 18ß(H)-oleanane (**II**) is unlikely and suggests either co-
587 elution or concentration below the detection limit.
588 Taraxastane (**XXI**), also a biomarker for land plant input (Nytoft et al.,
589 2010), was found to elute later in the first as well as second dimension
590 compared to α,ß-hopane, moretane and oleanane (**I**).

591 The concentrations of oleanane (**I** and **II**) plus lupane (**III**) correlate with
592 taraxastane (**XXI**) for all samples, supporting a similar source for all of
593 these compounds. The ratio of the sum of oleanane (**I** and **II**) and lupane
594 (**III**) to taraxastane (**XXI**) however is not constant. A correlation between
595 this ratio and maturity, age, the biodegradation level or latitude of the
596 sample was not found. The highest concentrations were determined in oil C2
597 and extract S5. Oleanane (**I** / **II**), lupane (**III**) or taraxastane (**XXI**) were not
598 detected in the marine condensate CA, rock S3 and coal S8. The coal was
599 already shown to have major land plant organic matter. The lack of
600 saturated pentacyclic angiosperm biomarkers supports immaturity as well
601 as diagenetic pathways favouring ring A-degraded and aromatised products.
602 A number of different C_{28}- and C_{29}- triterpenoids were identified and several
603 co-elution problems were resolved by GC×GC-TOFMS (Fig. 10). The 25-
604 norhopane series in biodegraded samples does not interfere with higher
605 plant derived saturated C_{28}- and C_{29}-compounds, as it elutes earlier in the
606 second dimension. 17ß(H)-24,28-bisnorlupane (**XXIII**) and 28,30-
607 bisnorhopane as well as 24-norlupane (**XXIV**) and 30-norhopane were
608 successfully resolved in the second dimension (Fig. 10). The compound co-
609 eluting with norhopane and norlupane (**XXIV**) is very similar to bisnor-
610 oleanane (**XXV**). Thus, it was tentatively identified as
611 bisnorursane/taraxastane (**XXVI**) based on its mass spectrum and the
612 elution order compared to first and second dimension retention times of the
613 des-A-counterparts (Fig. 10). The mass spectrum of the unidentified

614 compound eluting just above 17ß(H)-bisnorlupane (**XXIII**) is also similar to
615 bisnoroleanane (**XXV**) and bisnorursane/taraxastane (**XXVI**).
616 Relatively high concentrations of 17α(H)- and 17ß(H)-24,28-bisnorlupane
617 (**XXIII** and **XXVII**) and 24,28-bisnoroleanane (**XXV**) occur in most Arctic
618 oils and rock extracts. Bisnorlupanes and norlupanes are important
619 angiosperm biomarkers that have been applied to distinguish oil families in
620 Tertiary basins (Brooks, 1986; Curiale, 2006; Rullkötter et al., 1982;
621 Snowdon et al., 2004). The co-elution of 24,28-bisnorlupane (**XXIII**) and 24-
622 norlupane (**XXIV**) with 28,30-bisnorhopane and 30-norhopane, respectively,
623 in traditional 1D GC analysis was noted before (Curiale, 1991).
624 Quantification was especially difficult as both biomarkers yield abundant
625 mass fragments at *m/z* 177 and *m/z* 191. A correction factor calculated by
626 comparison of the relative abundances of *m/z* 177 and *m/z* 191 from
627 bisnorlupanes (**XXIII** and **XXVII**) and bisnorhopane was used to separate
628 oil families in the Beaufort-Mackenzie Basin (Curiale, 1991) based on the
629 presence or absence of these compounds. GC×GC-TOFMS resolves this co-
630 elution and allows reliable quantification. Our data support the distinction
631 established by Curiale et al. (2005) because all samples from Southeast Asia
632 are from onshore wells and lack bisnorlupanes (**XXIII**).
633 The broadest spectrum of unsaturated triterpenoids was observed in the
634 most immature rock. Mono- and di-unsaturated plant-derived pentacyclic
635 triterpenoids are commonly only present during early stages of diagenesis
636 as they are directly derived from amyrin by dehydration (Murray et al.,

637 1997; ten Haven et al., 1992a; ten Haven et al., 1992b; ten Haven and
638 Rullkötter, 1988). These compounds are thermally unstable and thus
639 rearrange to more stable aromatic or saturated products. The close elution
640 of these compounds requires the second dimension separation provided by
641 GC×GC to completely resolve all peaks. Furthermore, the sensitivity and
642 resolution of GC×GC resolves more mono-unsaturated triterpenoids than
643 were detected by traditional 1D GC, including isomers of known compounds
644 as well as potentially new biomarkers. This is true for all previously
645 discussed compound classes.
646 Many unsaturated triterpenoids are thermally unstable and prone to
647 rearrangement. Taraxer-14-ene (**XXVIII**), for example, co-elutes with n-C_{30}
648 alkane when analysed by GC-MS. However, exposure to common molecular
649 sieving procedures to remove n-alkanes (Grice et al., 2008) activates
650 rearrangement of taraxer-14-ene to a mixture of oleanene isomers
651 (Rullkötter et al., 1994). GC×GC separates such unstable compounds
652 without any required liquid chromatography or sieving steps prior to the
653 analysis. This is of particular importance to maintain the natural
654 distribution of biomarkers in the sample. Similarly, argentation
655 chromatography of non-polar fractions obtained from liquid chromatography
656 into saturated and unsaturated compounds can result in rearrangements of
657 double bonds in the olefins. None of these pre-separation steps are
658 necessary for GC×GC analysis, thus making this a valuable tool for analysis
659 of unstable compounds.

660 Aromatised pentacyclic oleanoids, ursanoids and lupanoids are well resolved
661 in the second dimension, like the aromatised des-A-compounds, which show
662 rapidly increasing ^2t_R for each additional aromatic ring in the structure.
663 Most abundant are tetra-aromatic ursanoids and oleanoids ($M^+ = 324$)
664 (Wakeham et al., 1980) in the oil samples, supporting advanced maturity
665 with progressive aromatisation (Freeman et al., 1994). As discussed before,
666 rock extract S10 contains, in addition to the unsaturated triterpenoids, high
667 concentrations of two 24,25,26,27-tetranor-oleanana(ursa)-
668 1,3,5(10),6,8,11,13-heptaenes (triaromatic pentacyclic oleanoid and
669 ursanoid, **XIV**) and a 24,25,26,27-tetranor-lupa-1,3,5(10),6,8,11,13-heptaene
670 (**XXIX**) (Jacob et al., 2007) as well as the tetraaromatic counterparts 1,2,9-
671 (ursane series, **XII**) and 2,2,9-trimethyl-1,2,3,4-tetrahydropicene (oleanane
672 series, **XIII**). In addition, the A, B, D-ring aromatised seco-oleanane (**XXX**)
673 and seco-lupane (**XXXI**) were identified (Chaffee and Fookes, 1988), eluting
674 considerably earlier in the first (14.5 min) and second (1 s) dimension than
675 the pentacyclic triaromatic oleanane and lupane, closer to the elution region
676 of other tetracyclic compounds.

677 *3.6.3 Relevance of land plant derived biomarkers*

678 The accurate separation, identification and quantification of plant
679 biomarkers is important because they provide valuable information about
680 the terrigenous source of organic matter in geological samples (Peters et al.,
681 2005a). Furthermore, angiosperm derived oleanoids, lupanoids and

682 ursanoids/taraxastoids are important age-diagnostic biomarkers for the
683 Late Cretaceous and younger, when flowering plants proliferated. The age
684 of the reservoir generally does not correspond to the age of the oil. In fact,
685 many oils migrate stratigraphically upward or even downward from their
686 source rock. Estimation of the age of oil solely based on geochemical
687 characteristics would be advantageous (Curiale, 2008). Eiserbeck (2011)
688 presented a tool for high resolution (within 10 Ma) age estimation of
689 Tertiary oils based on a ratio of extended angiosperm and gymnosperm
690 biomarkers. Improved and much more accurate separation and
691 quantification of these biomarkers is expected to equally improve the age
692 determination.
693 It was already shown that the presence or absence of plant biomarkers such
694 as 24,28-bisnorlupanes (**XXIII**, **XXVII**) can be used to help categorise oils
695 according to their source (Curiale, 1991). GC×GC improves assessment of
696 not only the occurrence of certain age- and source-related biomarkers, but
697 enhances our ability to compare individual isomers and concentrations of
698 compounds like lupane (**III**) or 24,28-bisnorlupane (**XXIII**) to allow more
699 refined correlations.
700 Different diagenetic and catagenetic pathways of higher plant biomarkers
701 like oleanoids were shown to result in various products (Murray et al.,
702 1997). Triterpenes are the key intermediates in the diagenetic pathway of
703 the naturally occurring amyrin towards progressively aromatised
704 pentacyclics, ring A-degraded tetracyclics, saturated pentacyclics or ring A-

705 contracted triterpenoids. Generally, oleanenes occur only in immature rocks
706 as they are rapidly transformed during maturation (Murray et al., 1997; ten
707 Haven and Rullkötter, 1988). Therefore, their occurrence in oils is commonly
708 explained by migration contamination. One Hammerhead oil from North
709 Alaska was reported with indigenous oleanene, apparently because it was
710 generated at a temperature as low as 60 °C (Curiale, 1995). Another
711 exception is the Niger Delta where oleanenes were found to be stable up to
712 the onset of petroleum generation, which allowed a distinction between
713 onshore and offshore oils (Eneogwe et al., 2002). Offshore oils contain
714 indigenous oleanenes and thus were released during the early stages of oil
715 generation, whereas oleanenes were absent in the more mature onshore oils,
716 supporting the rearrangement/transformation of oleananes with
717 maturation. Resolution of a number of co-elutions of triterpenes by GC×GC
718 provides the opportunity to better understand relationships between
719 maturity and the formation of distinct diagenetic products from plant
720 derived biological precursors.

4 Conclusions

This study demonstrates the superior resolution of land plant biomarkers provided by GC×GC compared to traditional 1D GC techniques like GC-MS or GC-MRM-MS. Table 3 summarises the most important conclusions. It was shown that some degree of co-elution occurs in 1D analysis in all studied compound classes– namely hopanoids, steroids, tricyclics, tetracyclic and pentacyclic land plant biomarkers. These compounds were successfully resolved in the second dimension using GC×GC analysis. Only one analysis was required on whole crude oils or source rock extracts in order to achieve baseline separation for these commonly low abundant higher plant markers. This is particularly important for the analysis of unstable components (e.g. unsaturated triterpenoids like taraxer-14-ene) that are prone to rearrangement when fractionated prior to the analysis (as in molecular sieving). Whole sample measurement using GC×GC maintains the natural distribution of such compounds without losing chromatographic resolution. GC×GC-FID results in improved peak shape, reproducibility and quantitative peak areas, while GC×GC-TOFMS analysis provides high resolution separation with access to full mass spectra throughout the chromatogram. Critical 1D GC separation problems that were resolved by GC×GC in $^{2}t_{R}$ include the co-elution of 24-norlupane and norhopane as well as 24,28-bisnorlupane and bisnorhopane, monoaromatic des-A-compounds (M^+ 310) and triaromatic pentacyclic triterpenoids (M^+ 342). Regular

743 steranes were separated in ^2t_R from diasteranes as well as bicadinanes, all
744 sharing a 217 mass fragment. Furthermore, enhanced sensitivity and
745 improved separation revealed co-elution problems that were not apparent
746 with traditional 1D GC such as the three compounds 1-3 co-eluting with
747 17α,21ß-hopane. Additional compounds were detected that had not been
748 observed by traditional GC-MS due to their low abundance in complex
749 mixtures like crude oil. Furthermore, components with identical molecular
750 masses and fragmentation patterns were resolved in the second GC
751 dimension, for instance the C_{24} des-A- and C_{23} nor-des-A-series (e.g. des-A-
752 lupane and nor-des-A-U/T), or the co-elution of des-A-lupene and des-A-
753 lupadiene with two isomers. These compounds were impossible to identify or
754 quantify using 1D GC techniques.
755 C_{32} homohopane isomerisation ratios from GC-MS, GC-MRM-MS, GC×GC-
756 FID and GC×GC-TOFMS compare well. Assessment of maturity using
757 GC×GC is compatible with older techniques and can be applied in
758 comparisons with the substantial amount of knowledge obtained in the past.
759 A series of Tertiary oils and rocks showed varying contributions of higher
760 plant derived organic matter. Differences in molecular distribution
761 depending on age, origin and maturity of the geological sample were
762 revealed and discussed. Consistent with its age, S1 is dominated by conifer
763 markers. S9 and S10 (Brunei) show an exceptional variety of unsaturated
764 angiosperm markers in agreement with their immaturity. Significantly
765 more unsaturated triterpenoids were observed in the GC×GC-TOFMS

766 analysis compared to 1D GC. Indigenous immature signals in S10 (e.g.
767 20Rααα sterane) are accompanied by abundant mature, aromatic higher
768 plant markers indicating migration contamination.
769 An unusual distribution of des-A-triterpenoids was identified in S8, which
770 consists almost exclusively of an unidentified des-A-compound 5. The lack of
771 pentacyclic plant triterpenoids suggests diagenetic pathways in favour of
772 ring A-degraded and aromatised products.

Acknowledgements: We thank Chevron Energy Technology Company for providing the sample material and also financial support. C.E. acknowledges Chevron, WA-Organic and Isotope Geochemistry Centre, European Association of Organic Geochemistry for a travel award, and Curtin University, The Institute for Geoscience Research (TIGeR), and WA Energy Research Alliance for funding. Geoff Chidlow is thanked for technical support. H.P. Nytoft is thanked for providing the 24,28-bisnorlupane standard. K. Peters and an anonymous reviewer are thanked for their helpful suggestions to improve this manuscript. K.G. acknowledges Australian Research Council Discovery series for funding. C.R. and R.N. thank the Seaver Institute and US Department of Energy. J.C. thanks Chevron for permission to publish.

784

785 **References**

786 Adahchour, M., Beens, J., and Brinkman, U. A. T., 2008. Recent
787 developments in the application of comprehensive two-dimensional
788 gas chromatography. *J. Chromatogr. A* **1186**, 67-108.
789 Adahchour, M., Beens, J., Vreuls, R. J. J., and Brinkman, U. A. T., 2006.
790 Recent developments in comprehensive two-dimensional gas
791 chromatography (GC×GC): IV. Further applications, conclusions and
792 perspectives. *TrAC, Trends Anal. Chem.* **25**, 821-840.
793 Aguiar, A., Silva Júnior, A. I., Azevedo, D. A., and Aquino Neto, F. R., 2010.
794 Application of comprehensive two-dimensional gas chromatography
795 coupled to time-of-flight mass spectrometry to biomarker
796 characterization in Brazilian oils. *Fuel* **89**, 2760-2768.
797 Alexander, R., Kagi, R. I., Noble, R., and Volkman, J. K., 1984.
798 Identification of some bicyclic alkanes in petroleum. *Org. Geochem.* **6**,
799 63-72.
800 Ames, T., Beton, J., Bowers, A., Halsall, T., and Jones, E., 1954. The
801 chemistry of the triterpenes and related compounds. Part XXIII. The
802 structure of taraxasterol, -taraxasterol (heterolupeol), and lupenol-I.
803 *J. Chem. Soc.*, 1905-1919.
804 Anderson, K. B. and Muntean, J. V., 2000. The nature and fate of natural
805 resins in the geosphere. Part X. Structural characteristics of the
806 macromolecular constituents of modern Dammar resin and Class II
807 ambers. *Geochem. Trans.* **1**, 1-9.
808 Bennett, B., Fustic, M., Farrimond, P., Huang, H., and Larter, S. R., 2006.
809 25-Norhopanes: Formation during biodegradation of petroleum in the
810 subsurface. *Org. Geochem.* **37**, 787-797.
811 Brooks, P. W., 1986. Unusual biological marker geochemistry of oils and
812 possible source rocks, offshore Beaufort-Mackenzie Delta, Canada.
813 *Org. Geochem.* **10**, 401-406.
814 Chaffee, A. L. and Fookes, C. J. R., 1988. Polycyclic aromatic hydrocarbons
815 in Australian coals--III. Structural elucidation by proton nuclear
816 magnetic resonance spectroscopy. *Org. Geochem.* **12**, 261-271.
817 Crelling, J. C., Pugmire, R. J., Meuzelaar, H. L. C., McClennen, W. H., Huai,
818 H., and Karas, J., 1991. Chemical structure and petrology of resinite
819 from the Hiawatha" B" coal seam. *Energy & Fuels* **5**, 688-694.
820 Curiale, J., Lin, R., and Decker, J., 2005. Isotopic and molecular
821 characteristics of Miocene-reservoired oils of the Kutei Basin,
822 Indonesia. *Org. Geochem.* **36**, 405-424.
823 Curiale, J. A., 1991. The petroleum geochemistry of Canadian Beaufort
824 Tertiary "non-marine" oils. *Chem. Geol.* **93**, 21-45.
825 Curiale, J. A., 1995. Saturated and olefinic terrigenous triterpenoid
826 hydrocarbons in a biodegraded tertiary oil of northeast Alaska. *Org.*
827 *Geochem.* **23**, 177-182.

828 Curiale, J. A., 2006. The occurrence of norlupanes and bisnorlupanes in oils
829 of Tertiary deltaic basins. *Org. Geochem.* **37**, 1846-1856.
830 Curiale, J. A., 2008. Oil-source rock correlations - Limitations and
831 recommendations. *Org. Geochem.* **39**, 1150-1161.
832 Dawson, D., Grice, K., and Alexander, R., 2005. Effect of maturation on the
833 indigenous δD signatures of individual hydrocarbons in sediments
834 and crude oils from the Perth Basin (Western Australia). *Org.*
835 *Geochem.* **36**, 95-104.
836 Dimandja, J. M. D., 2004. GC x GC. *Anal. Chem.* **76**, 167A-174A.
837 Eglinton, G. and Hamilton, R. J., 1967. Leaf epicuticular waxes. *Science*
838 **156**, 1322-1335.
839 Eiserbeck, C., 2011. Molecular and isotope chronostratigraphy of Tertiary
840 source rocks and crude oils, Curtin University.
841 Eiserbeck, C., Nelson, R. K., Grice, K., Curiale, J., Reddy, C. M., and Raiteri,
842 P., 2011. Separation of 18α(H)-, 18ß(H)-oleanane and lupane by
843 comprehensive two-dimensional gas chromatography. *J. Chromatogr.*
844 *A* **1218**, 5549-5553.
845 Ekweozor, C. M. and Udo, O. T., 1988. The oleananes: Origin, maturation
846 and limits of occurence in Southern Nigeria sedimentary basins. *Org.*
847 *Geochem.* **13**, 131-140.
848 Eneogwe, C., Ekundayo, O., and Patterson, B., 2002. Source-derived
849 oleanenes identified in Niger Delta oils. *Journal of Petroleum Geology*
850 **25**, 83-95.
851 Freeman, K. H., Boreham, C. J., Summons, R. E., and Hayes, J. M., 1994.
852 The effect of aromatization on the isotopic compositions of
853 hydrocarbons during early diagenesis. *Org. Geochem.* **21**, 1037-1049.
854 Frysinger, G. S. and Gaines, R. B., 2001. Separation and identification of
855 petroleum biomarkers by comprehensive two-dimensional gas
856 chromatography. *J. Sep. Sci.* **24**, 87-96.
857 Frysinger, G. S., Gaines, R. B., Xu, L., and Reddy, C. M., 2003. Resolving
858 the unresolved complex mixture in petroleum-contaminated
859 sediments. *Environmental Science & Technology* **37**, 1653-1662.
860 Gaines, R. B., Frysinger, G. S., Hendrick-Smith, M. S., and Stuart, J. D.,
861 1999. Oil spill source identification by comprehensive two-
862 dimensional gas chromatography. *Environmental Science &*
863 *Technology* **33**, 2106-2112.
864 Gaines, R. B., Frysinger, G. S., Reddy, C. M., and Nelson, R. K., 2006. Oil
865 Spill Source Identification by Comprehensive Two-dimensional Gas
866 Chromatography (GC × GC). In: Wang, Z. and Stout, S. Eds.), *Spill*
867 *Oil Fingerprinting and Source Identification*. Academic Press, New
868 York.
869 Gelpi, E., Schneider, H., Mann, J., and Oro, J., 1970. Hydrocarbons of
870 geochemical significance in microscopic algae. *Phytochemistry* **9**, 603-
871 612.
872 Giddings, J. C., 1984. Two-dimensional separations - concept and promise.
873 *Anal. Chem.* **56**, 1258-1270.

874 Grice, K., Mesmay, R. d., Glucina, A., and Wang, S., 2008. An improved and
875 rapid 5A molecular sieve method for gas chromatography isotope
876 ratio mass spectrometry of *n*-alkanes (C_8-C_{30}+). *Org. Geochem.* **39**,
877 284-288.
878 Grice, K., Schaeffer, P., Schwark, L., and Maxwell, J. R., 1997. Changes in
879 palaeoenvironmental conditions during deposition of the Permian
880 Kupferschiefer (Lower Rhine Basin, northwest Germany) inferred
881 from molecular and isotopic compositions of biomarker components.
882 *Org. Geochem.* **26**, 677-690.
883 Huang, X., Xie, S., Zhang, C. L., Jiao, D., Huang, J., Yu, J., Jin, F., and Gu,
884 Y., 2008. Distribution of aliphatic des-A-triterpenoids in the Dajiuhu
885 peat deposit, southern China. *Org. Geochem.* **39**, 1765-1771.
886 Huang, Y., Lockheart, M. J., Collister, J. W., and Eglinton, G., 1995.
887 Molecular and isotopic biogeochemistry of the Miocene Clarkia
888 Formation: hydrocarbons and alcohols. *Org. Geochem.* **23**, 785-801.
889 Jacob, J., Disnar, J.-R., Boussafir, M., Spadano Albuquerque, A. L.,
890 Sifeddine, A., and Turcq, B., 2007. Contrasted distributions of
891 triterpene derivatives in the sediments of Lake Caco reflect
892 paleoenvironmental changes during the last 20,000 yrs in NE Brazil.
893 *Org. Geochem.* **38**, 180-197.
894 Lemkau, K. L., Peacock, E. E., Nelson, R. K., Ventura, G. T., Kovecses, J. L.,
895 and Reddy, C. M., 2010. The M/V Cosco Busan spill: Source
896 identification and short-term fate. *Marine Pollution Bulletin* **60**,
897 2123-2129.
898 Li, M., Zhang, S., Jiang, C., Zhu, G., Fowler, M., Achal, S., Milovic, M.,
899 Robinson, R., and Larter, S., 2008. Two-dimensional gas
900 chromatograms as fingerprints of sour gas-associated oils. *Org.*
901 *Geochem.* **39**, 1144-1149.
902 Logan, G. A. and Eglinton, G., 1994. Biogeochemistry of the Miocene
903 lacustrine deposit, at Clarkia, northern Idaho, U.S.A. *Org. Geochem.*
904 **21**, 857-870.
905 Mackenzie, A. S., Brassell, S. C., Eglinton, G., and Maxwell, J. R., 1982.
906 Chemical fossils - the geological fate of steroids. *Science* **217**, 491-504.
907 Maslen, E., Grice, K., Gale, J. D., Hallmann, C., and Horsfield, B., 2009.
908 Crocetane: A potential marker of photic zone euxinia in thermally
909 mature sediments and crude oils of Devonian age. *Org. Geochem.* **40**,
910 1-11.
911 Moldowan, J. M., Dahl, J., Huizinga, B. J., Fago, F. J., Hickey, L. J.,
912 Peakman, T. M., and Taylor, D. W., 1994. The molecular fossil record
913 of oleanane and its relation to angiosperms. *Science* **265**, 768-771.
914 Morley, R. J., 2000. *Origin and evolution of tropical rain forests*. Wiley-
915 Blackwell, New York.
916 Murray, A. P., Sosrowidjojo, I. B., Alexander, R., Kagi, R. I., Norgate, C. M.,
917 and Summons, R. E., 1997. Oleananes in oils and sediments:
918 Evidence of marine influence during early diagenesis? *Geochim.*
919 *Cosmochim. Acta* **61**, 1261-1276.

Murray, A. P., Summons, R. E., Boreham, C. J., and Dowling, L. M., 1994. Biomarker and *n*-alkane isotope profiles for Tertiary oils: relationship to source rock depositional setting. *Org. Geochem.* **22**, 521-542, IN5-IN6.

Nelson, R. K., Kile, B. M., Plata, D. L., Sylva, S. P., Xu, L., Reddy, C. M., Gaines, R. B., Frysinger, G. S., and Reichenbach, S. E., 2006. Tracking the Weathering of an Oil Spill with Comprehensive Two-Dimensional Gas Chromatography. *Environmental Forensics* **7**, 33 - 44.

Noble, R. A., Alexander, R., Kagi, R. I., and Knox, J., 1985. Tetracyclic diterpenoid hydrocarbons in some Australian coals, sediments and crude oils. *Geochim. Cosmochim. Acta* **49**, 2141-2147.

Noble, R. A., Alexander, R., Kagi, R. I., and Knox, J. K., 1986. Identification of some diterpenoid hydrocarbons in petroleum. *Org. Geochem.* **10**, 825-829.

Nytoft, H. P., Bojesen-Koefoed, J. A., Christiansen, F. G., and Fowler, M. G., 2002. Oleanane or lupane? Reappraisal of the presence of oleanane in Cretaceous-Tertiary oils and sediments. *Org. Geochem.* **33**, 1225-1240.

Nytoft, H. P., Kildahl-Andersen, G., and Samuel, O. J., 2010. Rearranged oleananes: Structural identification and distribution in a worldwide set of Late Cretaceous/Tertiary oils. *Org. Geochem.* **41**, 1104-1118.

Otto, A. and Wilde, V., 2001. Sesqui-, di-, and triterpenoids as chemosystematic markers in extant conifers- A review. *Botanical Review* **67**, 141-238.

Perkins, G. M., Bull, I. D., Ten Haven, H. L., Rullkötter, J., Smith, Z. E. F., and Peakman, T. M., 1995. First positive identification of triterpanes of the taraxastane family in petroleums and oil shales: 19α(H)-taraxastane and 24-nor-19α(H)-taraxastane. Evidence for a previously unrecognised diagenetic alteration pathway of lup-20(29)-ene derivatives. In: Grimalt, J. O., Dorronsoro, C. (Eds.) (Ed.),*Selected papers from the 17th International Meeting on Organic Geochemistry* Donastia-San Sebastián, The Basque Country. Spain.

Peters, K. E., Moldowan, J. M., McCaffrey, M. A., and Fago, F. J., 1996. Selective biodegradation of extended hopanes to 25-norhopanes in petroleum reservoirs. Insights from molecular mechanics. *Org. Geochem.* **24**, 765-783.

Peters, K. E., Walters, C. C., and Moldowan, J. M., 2005a. *The Biomarker Guide*. Cambridge University Press, Cambridge.

Peters, K. E., Walters, C. C., and Moldowan, J. M., 2005b. *The Biomarker Guide, Volume 2: Biomarkers and Isotopes in Petroleum Exploration and Earth History*. Cambridge University Press, Cambridge.

Philp, R. P. and Gilbert, T. D., 1986. Biomarker distributions in Australian oils predominantly derived from terrigenous source material. *Org. Geochem.* **10**, 73-84.

965 Riva, A., Caccialanza, P. G., and Quagliaroli, F., 1988. Recognition of
966 18β(H)-oleanane in several crudes and Tertiary-Upper Cretaceous
967 sediments. Definition of a new maturity parameter. *Org. Geochem.*
968 **13**, 671-675.
969 Rullkötter, J., Leythaeuser, D., and Wendisch, D., 1982. Novel 23,28-
970 bisnorlupanes in Tertiary sediments. Widespread occurrence of
971 nuclear demethylated triterpanes. *Geochim. Cosmochim. Acta* **46**,
972 2501-2509.
973 Rullkötter, J., Peakman, T. M., and Ten Haven, H. L., 1994. Early
974 diagenesis of terrigenous triterpenoids and its implications for
975 petroleum geochemistry. *Org. Geochem.* **21**, 215-233.
976 Samuel, O. J., Kildahl-Andersen, G., Nytoft, H. P., Johansen, J. E., and
977 Jones, M., 2010. Novel tricyclic and tetracyclic terpanes in Tertiary
978 deltaic oils: Structural identification, origin and application to
979 petroleum correlation. *Org. Geochem.* **41**, 1326-1337.
980 Sandison, C. M., 2001. The Organic Geochemistry of Marine-Influenced
981 Coals, Curtin University of Technology.
982 Silva, R. S. F., Aguiar, H. G. M., Rangel, M. D., Azevedo, D. A., and Aquino
983 Neto, F. R., 2011. Comprehensive two-dimensional gas
984 chromatography with time of flight mass spectrometry applied to
985 biomarker analysis of oils from Colombia. *Fuel* **90**, 2694-2699.
986 Smith, Z. E. F., 1995. Characterisation of A-ring contracted triterpenoids in
987 oils and shales: Evidence for an alternative transformation pathway
988 in the diagenesis of higher plant triterpenoids., University of Bristol.
989 Snowdon, L. R., Stasiuk, L. D., Robinson, R., Dixon, J., Dietrich, J., and
990 McNeil, D. H., 2004. Organic geochemistry and organic petrology of a
991 potential source rock of early Eocene age in the Beaufort-Mackenzie
992 Basin. *Org. Geochem.* **35**, 1039-1052.
993 Stefanova, M., Ivanov, D., Yaneva, N., Marinov, S., Grasset, L., and Amblès,
994 A., 2008. Palaeoenvironment assessment of Pliocene Lom lignite
995 (Bulgaria) from bitumen analysis and preparative off line
996 thermochemolysis. *Org. Geochem.* **39**, 1589-1605.
997 Stout, S. A., 1992. Aliphatic and aromatic triterpenoid hydrocarbons in a
998 Tertiary angiospermous lignite. *Org. Geochem.* **18**, 51-66.
999 ten Haven, H. L., Lafargue, E., and Kotarba, M., 1993. Oil/oil and oil/source
1000 rock correlations in the Carpathian Foredeep and Overthrust, south-
1001 east Poland. *Org. Geochem.* **20**, 935-959.
1002 ten Haven, H. L., Peakman, T. M., and Rullkötter, J., 1992a. Δ^2-Triterpenes:
1003 Early intermediates in the diagenesis of terrigenous triterpenoids.
1004 *Geochim. Cosmochim. Acta* **56**, 1993-2000.
1005 ten Haven, H. L., Peakman, T. M., and Rullkötter, J., 1992b. Early
1006 diagenetic transformation of higher-plant triterpenoids in deep-sea
1007 sediments from Baffin Bay. *Geochim. Cosmochim. Acta* **56**, 2001-
1008 2024.
1009 ten Haven, H. L. and Rullkötter, J., 1988. The diagenetic fate of taraxer-14-
1010 ene and oleanene isomers. *Geochim. Cosmochim. Acta* **52**, 2543-2548.

1011 Tissot, B. and Welte, D., 1984. *Petroleum Formation and Occurrence*
1012 Springer, Berlin Heidelberg New York.
1013 Tran, T. C., Logan, G. A., Grosjean, E., Harynuk, J., Ryan, D., and Marriott,
1014 P., 2006. Comparison of column phase configurations for
1015 comprehensive two dimensional gas chromatographic analysis of
1016 crude oil and bitumen. *Org. Geochem.* **37**, 1190-1194.
1017 Tran, T. C., Logan, G. A., Grosjean, E., Ryan, D., and Marriott, P. J., 2010.
1018 Use of comprehensive two-dimensional gas chromatography/time-of-
1019 flight mass spectrometry for the characterization of biodegradation
1020 and unresolved complex mixtures in petroleum. *Geochim.*
1021 *Cosmochim. Acta* **74**, 6468-6484.
1022 van Aarssen, B. G. K., Cox, H. C., Hoogendoorn, P., and de Leeuw, J. W.,
1023 1990a. A cadinene biopolymer in fossil and extant dammar resins as a
1024 source for cadinanes and bicadinanes in crude oils from South East
1025 Asia. *Geochim. Cosmochim. Acta* **54**, 3021-3031.
1026 van Aarssen, B. G. K., de Leeuw, J. W., Collinson, M., Boon, J. J., and Goth,
1027 K., 1994. Occurrence of polycadinene in fossil and recent resins.
1028 *Geochim. Cosmochim. Acta* **58**, 223-229.
1029 van Aarssen, B. G. K., Kruk, C., Hessels, J. K. C., and de Leeuw, J. W.,
1030 1990b. Cis-cis-trans-bicadinane, a novel member of an uncommon
1031 triterpane family isolated from crude oils. *Tetrahedron Lett.* **31**, 4645-
1032 4648.
1033 Ventura, G. T., Hall, G. J., Nelson, R. K., Frysinger, G. S., Raghuraman, B.,
1034 Pomerantz, A. E., Mullins, O. C., and Reddy, C. M., 2011. Analysis of
1035 petroleum compositional similarity using multiway principal
1036 components analysis (MPCA) with comprehensive two-dimensional
1037 gas chromatographic data. *J. Chromatogr. A* **1218**, 2584-2592.
1038 Ventura, G. T., Kenig, F., Reddy, C. M., Frysinger, G. S., Nelson, R. K.,
1039 Mooy, B. V., and Gaines, R. B., 2008. Analysis of unresolved complex
1040 mixtures of hydrocarbons extracted from Late Archean sediments by
1041 comprehensive two-dimensional gas chromatography (GC×GC). *Org.*
1042 *Geochem.* **39**, 846-867.
1043 Ventura, G. T., Kenig, F., Reddy, C. M., Schieber, J., Frysinger, G. S.,
1044 Nelson, R. K., Dinel, E., Gaines, R. B., and Schaeffer, P., 2007.
1045 Molecular Evidence of Late Archean Archaea and the Presence of a
1046 Subsurface Hydrothermal Biosphere. *Proceedings of the National*
1047 *Academy of Sciences of the United States of America* **104**, 14260-
1048 14265.
1049 Ventura, G. T., Raghuraman, B., Nelson, R. K., Mullins, O. C., and Reddy,
1050 C. M., 2010. Compound class oil fingerprinting techniques using
1051 comprehensive two-dimensional gas chromatography (GC×GC). *Org.*
1052 *Geochem.* **41**, 1026-1035.
1053 Volkman, J. K., Alexander, R., Kagi, R. I., and Woodhouse, G. W., 1983.
1054 Demethylated hopanes in crude oils and their applications in
1055 petroleum geochemistry. *Geochim. Cosmochim. Acta* **47**, 785-794.

Volkman, J. K., Barrett, S. M., Blackburn, S. I., Mansour, M. P., Sikes, E. L., and Gelin, F., 1998. Microalgal biomarkers: A review of recent research developments. *Org. Geochem.* **29**, 1163-1179.

Wakeham, S. G., Schaffner, C., and Giger, W., 1980. Polycyclic aromatic hydrocarbons in Recent lake sediments--II. Compounds derived from biogenic precursors during early diagenesis. *Geochim. Cosmochim. Acta* **44**, 415-429.

Wang, F. C. Y. and Walters, C. C., 2007. Pyrolysis comprehensive chromatography study of two-dimensional gas petroleum source rock. *Anal. Chem.* **79**, 5642-5650.

Wenger, L. M. and Isaksen, G. H., 2002. Control of hydrocarbon seepage intensity on level of biodegradation in sea bottom sediments. *Org. Geochem.* **33**, 1277-1292.

Woolhouse, A. D., Oung, J. N., Philp, R. P., and Weston, R. J., 1992. Triterpanes and ring-A degraded triterpanes as biomarkers characteristic of Tertiary oils derived from predominantly higher plant sources. *Org. Geochem.* **18**, 23-31.

Zhou, Y., Sheng, G., Fu, J., Geng, A., Chen, J., Xiong, Y., and Zhang, Q., 2003. Triterpane and sterane biomarkers in the YA13-1 condensates from Qiongdongnan Basin, South China Sea. *Chem. Geol.* **199**, 343-359.

Zumberge, J. E., 1987. Prediction of source rock characteristics based on terpane biomarkers in crude oils: A multivariate statistical approach. *Geochim. Cosmochim. Acta* **51**, 1625-1637.

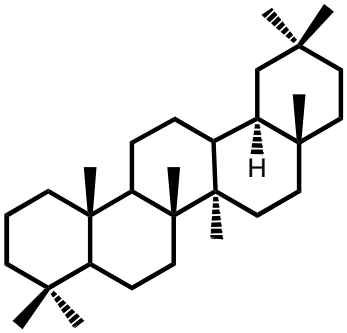

I
18α(H)-oleanane

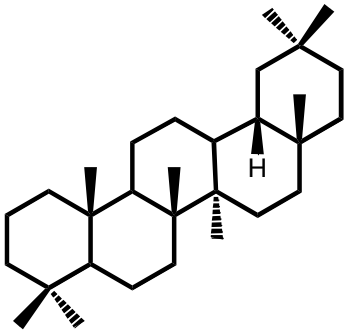

II
18β(H)-oleanane

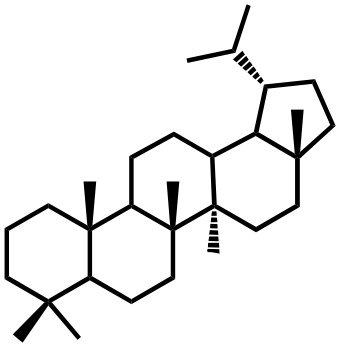

III
lupane

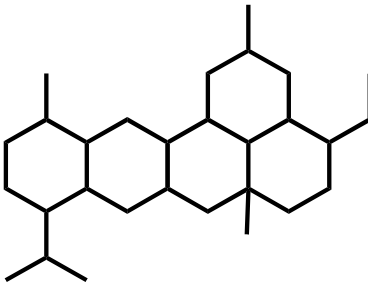

IV
bicadinane

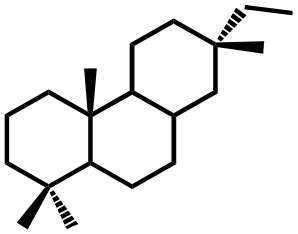

V
isopimarane

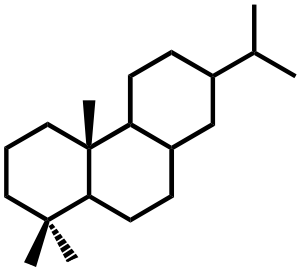

VI
abietane

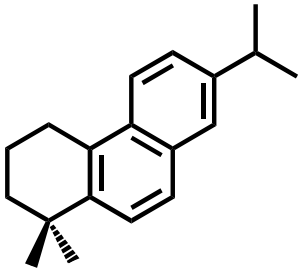

VII
simonellite

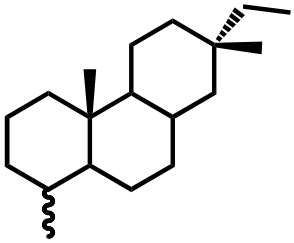

VIII
norisopimarane

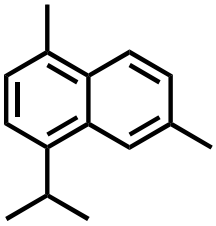

IX
cadalene

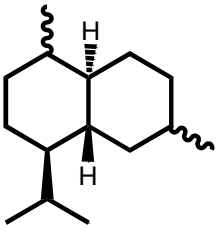

X
cadinane

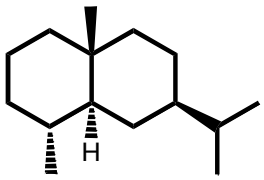

XI
eudesmane

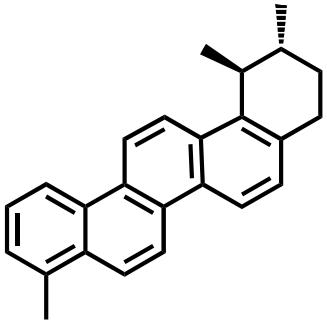

XII
1,2,9-trimethyl-1,2,3,4-tetrahydropicene

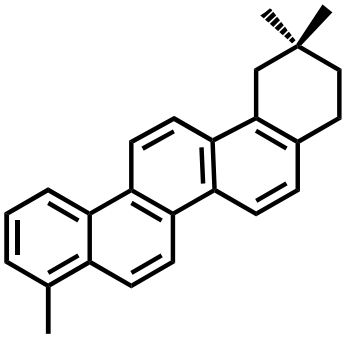

XIII
2,2,9-trimethyl-1,2,3,4-tetrahydropicene

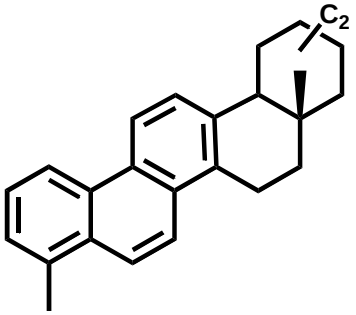

XIV
24, 25, 26, 27-tetranor-oleana(ursa)- 1, 3, 5(10), 6, 8, 11, 13-heptaene

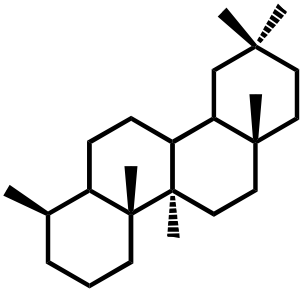

XV
des-A-oleanane

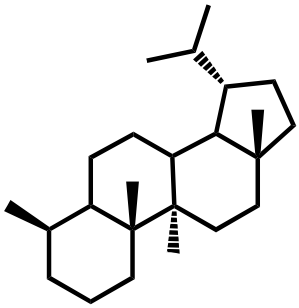

XVI
des-A-lupane

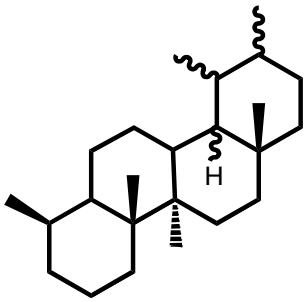

XVII
des-A-ursane/ taraxastane

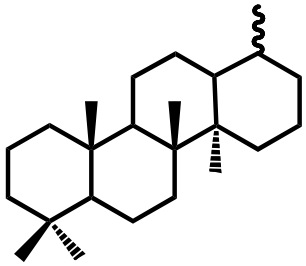

XVIII
des-E-hopane

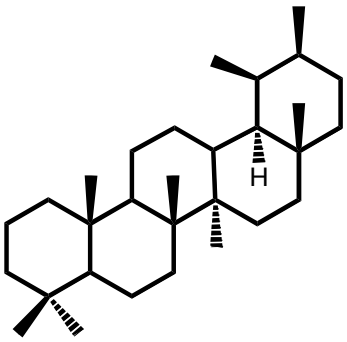

XIX
19α-taraxastane (a)

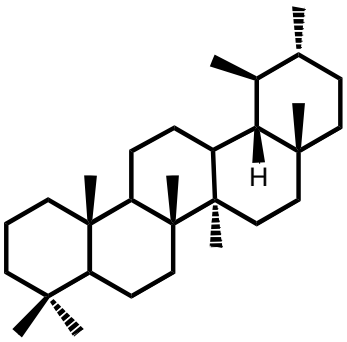

XX
ursane (a)

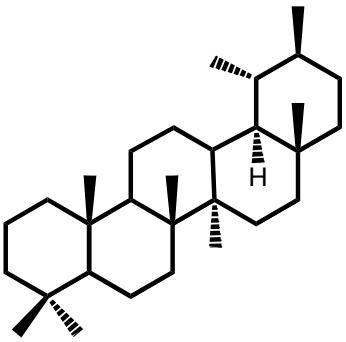

XXI
taraxastane (b)

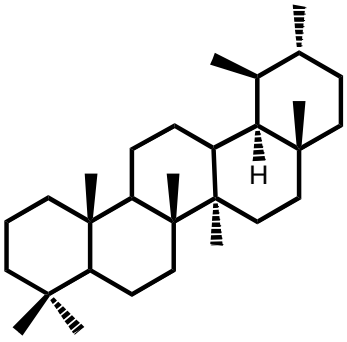

XXII
ursane (b)

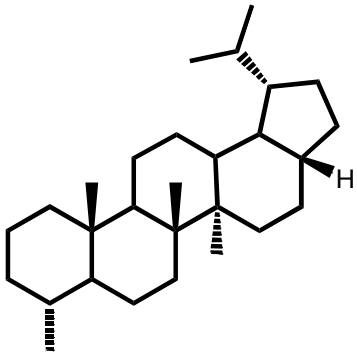

XXIII
17β-24, 28-bisnorlupane

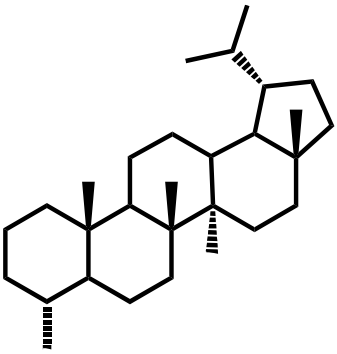

XXIV
24-norlupane

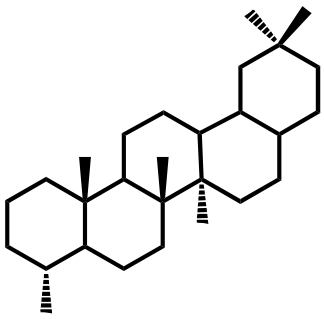

XXV
24, 28-bisnoroleanane

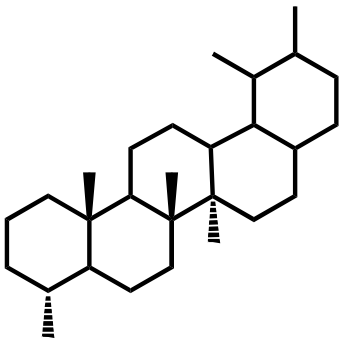

XXVI
24, 28-bisnorursane/ taraxastane

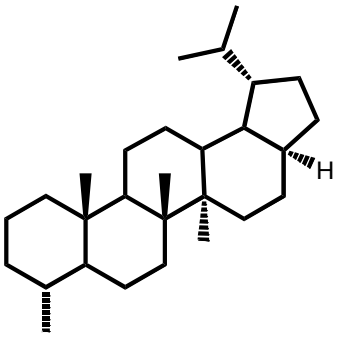

XXVII
17α-24, 28-bisnorlupane

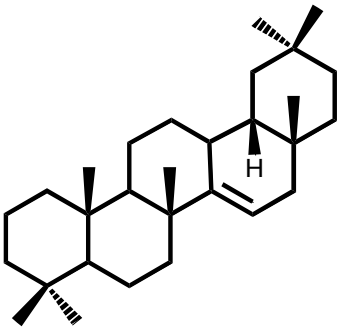

XXVIII
taraxer-14-ene

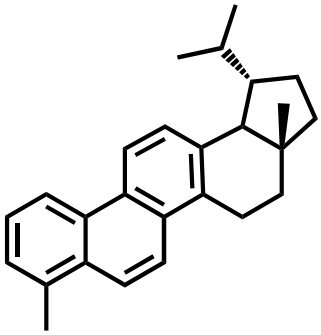

XXIX
24, 25, 26, 27-tetranor-lupa- 1, 3, 5(10), 6, 8, 11, 13- heptaene

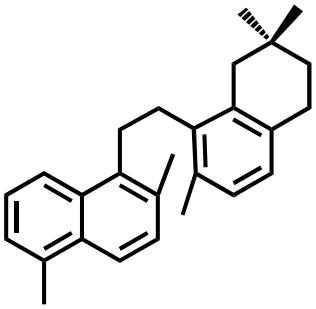

XXX

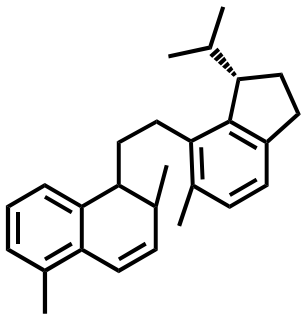

XXXI

1083
1084

Appendix 2

Selected ions (GC-MS SIM mode) and transitions (GC-MRM-MS) used to obtain the chromatograms shown in Fig. 4a and Fig. 4b.

selected ions included in GC-MS SIM mode	transitions included in MRM analysis	
	parent ion	daughter ion
219	412	397
205	398	383
191	384	369
177	374	359
163	412	369
412	398	355
123	384	341
149	412	274
189	398	260
175	412	259
276	374	220
262	374	219
247	398	191
218	412	191
396	384	177
410		
367		

Appendix 3

C_{32} homohopane 22*S*/(22*S*+22*R*) ratios determined for four techniques and their statistical evaluation including the average value of the ratio for each sample (AVE), the standard deviation of the ratio averages of each measure (STD), and the percentage that standard deviation presents of the average value (%).

sample	GC-MS	MRM	GCxGC-TOF	GCxGC-FID	AVE	STD	%
A1	0.58	0.57	0.60	0.58	0.59	0.01	2
A2	0.53	0.50	0.55	0.56	0.53	0.03	5
A3	0.45	0.43	0.45	0.52	0.46	0.04	8
C2	0.54	0.53	0.56	0.58	0.55	0.02	4
C3	0.54	0.56	0.56	0.57	0.56	0.01	2
C4	0.57	0.58	0.54	0.57	0.56	0.02	3
M1	0.62	0.58	0.63	0.61	0.61	0.02	3
M2	0.60	0.54	0.61	0.60	0.59	0.03	5
CA	n.d.	n.d.	n.d.	n.d.	n.d.	n.d.	n.d.
S1	0.50	0.48	0.54	0.49	0.50	0.03	5
S2	0.52	0.52	0.55	0.53	0.53	0.01	3
S3	0.60	0.55	0.61	0.59	0.59	0.03	4
S4	0.50	0.49	0.53	0.51	0.51	0.02	4
S5	0.38	0.41	0.48	0.44	0.43	0.04	10
S6	0.39	0.40	0.46	0.50	0.44	0.05	12
S7	0.58	0.56	0.61	0.59	0.58	0.02	4
S8	n.d.	n.d.	n.d.	n.d.	n.d.	n.d.	n.d.
S9	0.32	0.25	0.18	0.07	0.20	0.10	51
S10	0.11	0.07	0.03	0.03	0.06	0.04	67

Appendix 4

Selected ions (GC-MS and GCxGC-TOFMS) and transitions (GC-MRM-MS) used for identification and quantification of the biomarkers discussed in the manuscript. The first mass fragment commonly represents the molecular mass fragment, whereas fragments in bold were used for quantification.

1108

compound	SIM ions	MRM transitions		GCxGC ions
		parent ion	daughter ion	
hopanes, steranes				
C_{32} HH	440, **191**	440	191	440, **191**
αβ-,βα-hopanes	177, **191**	370/384/398/ 412/426/440/454	191	**191**, 177
ββ-hopanes	**205***	370/384/398/ 412/426/440/454	205	**205***
C_{29} steranes	400, **217**	400	217	**217***
diasteranes	**217**, 259*	372/386/400/414	**217**, 259	**217**, 259*
25-norhopanes	**177***	370/384/398/ 412/426/440	177	**177***
gymnosperm markers				
isopimarane, **V**	276, **247**, 191	276	191	**276**
abietane, **VI**	276, **163**	n.d.	n.d.	**276**
simonellite, **VII**	**237**	n.d.	n.d.	**237**
norisopimarane, **VIII**	262, **233**	262	191	262, **233**
saturated angiosperm markers				
18α(H)-oleanane, **I**	412, **191**	412	191	412, **191**
18β(H)-oleanane, **II**	412, **191**	412	191	412, **191**
lupane, **III**	412, 191, **369**	412	**191**, 369	412, 191, **369**
taraxastane, **XXI**	412, **191**	412	191	412, **191**
bicadinanes, **IV**	412, 369, 217	412	369	217, **369**
compound 1	n.d.	n.d.	n.d.	398, **191**, 177
compound 2	n.d.	n.d.	n.d.	398, **177**, 255
compound 3	n.d.	n.d.	n.d.	398, **191**, 355
24-norlupane, **XXIV**	398, 191, **177**, 355	398	**177**/ 355	398, 191, **177**, 355
17α(H)-24,28-bisnorlupane, **XXVII** 17β(H)-24,28-bisnorlupane, **XXIII**	384, **177**, 341	**384**	**177**/341	384, **177**, 341
24,28-bisnoroleanane, **XXV**	384, **177**	384	177	384, **177**
bisnorursane/taraxastane, **XXVI**	384, **177**	384	177	384, **177**
des-A-triterpenoids				
des-A-oleanane, **XV**	330, **191**, 177, 206, 315	330	191	330, **191,** 177, 206, 315
des-A-ursane/taraxastane, **XVII**	330, **177, 191**, 315, 206	330	191	330, **177**, 191, 315, 206
des-A-lupane, **XVI**	330, **287**, 163, 191, 177,206	330	**206**, 287	330, **287**, 163, 191, 177,206
des-E-hopane, **XVIII**	330, **191**, 177, 315	330	191	330, **191**, 177, 315
compound 5	330, **191**, 177, 206	330	206	330, 191, 177, 206
compound 6	330, **191**, 177, 315, 206	330	206	330, 191, 177, 315, 206
nor-des-A-U/T	316, **177**	316	177	316, **177**
unsaturated triterpenoids				
monounsaturated des-A-triterpenoids	328	n.d.	n.d.	328
des-A-lupene	328, 285	n.d.	n.d.	328, 285
compound 7	328	n.d.	n.d.	328
des-A-lupadiene	326, 283	n.d.	n.d.	326, 283
compound 8	326	n.d.	n.d.	326
diunsaturated des-A-triterpenoids	326	n.d.	n.d.	326
aromatics				
1,2,9-trimethyl-1,2,3,4-tetrahydropicene, **XII**	**324**, 209	n.d.	n.d.	**324**, 209
2,2,9-trimethyl-1,2,3,4-tetrahydropicene, **XIII**	**324**, 268	n.d.	n.d.	**324**, 268
24,25,26,27-tetranor-oleana(ursa)-1,3,5(10),6,8,11,13- heptaene, **XIV**	342, **257**	n.d.	n.d.	342, **257**
monoaromatic des-A-compounds	**310**	n.d.	n.d.	**310**
triaromatic pentacyclic triterpenoids	**342**	n.d.	n.d.	**342**

1109 * Molecular masses are equivalent to the parent ions shown for GC-MRM-MS transitions.

6 Tables

Table 1. Oils included in this study and their major biomarker characteristics.

sample name	Basin	reservoir age	biodegradation level [a]	biodegradation indicators	%C_{29} [b]	Dia/(Dia + Reg) steranes[d]	22S/(22S+22R) C_{32} hopanes[e]	ββ/(αα + ββ) C_{29} steranes[f]	20S/(20S+20R) C_{29} steranes[g]	Pr/Ph
A1	North Slope, Alaska	Mid-Tertiary	0	no biodegradation	51	0.48	0.57	0.47	0.33	2.34
A2	North Slope, Alaska	Mid-Tertiary	7	*n*-alkanes, isoprenoids, steranes completely removed, hopanes and tetramethylnaphthalenes partly degraded	n.d[c]	1.00	0.50	n.d[c]	n.d[c]	n.d[c]
A3	North Slope, Alaska	Mid-Tertiary	7	*n*-alkanes, isoprenoids, steranes completely removed, hopanes and tetramethylnaphthalenes partly degraded	n.d[c]	1.00	0.43	n.d[c]	n.d[c]	n.d[c]
C2	Canadian-Beaufort	Tertiary	1	*n*-alkanes partly degraded, UCM	71	0.36	0.53	0.36	0.14	3.11
C3	Canadian-Beaufort	Tertiary	3	*n*-alkanes and isoprenoids strongly degraded, UCM , methylnaphthalenes partly degraded	73	0.39	0.56	0.41	0.22	1.01[h]
C4	Canadian-Beaufort	Tertiary	0	no biodegradation	75	0.45	0.58	0.44	0.47	3.79
M1	central Myanmar	Oligocene	0	no biodegradation	69	0.39	0.58	0.54	0.50	5.27
M2	central Myanmar	Miocene	0	no biodegradation	62	0.37	0.54	0.54	0.54	4.81
CA	Santa Maria, California	Miocene	0	no biodegradation	16	0.23	0.51	0.50	0.55	0.93

[a] Peters et al. (2005b), Wenger and Isaksen (2002)
[b] C_{29} sterane percentage (in C_{27} – C_{29}) determined using GC-MRM-MS transition $M^+ \rightarrow 217$
[c] n.d.: complete removal or severe alteration of these compounds by biodegradation
[d] ratio determined from areas of GC-MRM-MS transitions $M^+ \rightarrow 217$ for C_{27} to C_{29} steranes

[e] based on areas of the GC-MRM-MS transition mass to charge ratio (m/z) 440 → 191
[f] calculated from the 20S and 20R C_{29} sterane areas of transition parent ion → 217
[g] calculated from the αααα-C_{29} sterane areas of transition parent ion → 217
[h] true value is masked by partly biodegraded isoprenoids

Table 2. Rock extracts included in this study.

sample name	Basin/ Origin	inferred source age	%C_{29} ($\alpha\alpha\alpha$+$\alpha\beta\beta$ S+R)[a]	Dia/(Dia + Reg) steranes[b]	22S/(22S+22R) C_{32} hopanes[c]	$\beta\beta$/($\alpha\alpha$ + $\beta\beta$) C_{29} steranes[e]	20S/(20S+20R) C_{29} steranes[f]	Pr/Ph
S1	North Slope, Alaska	Late Paleocene	30	0.28	0.48	0.46	0.21	1.51
S2	Canadian-Beaufort	Early Oligocene	49	0.46	0.52	0.33	0.22	1.86
S3	Canadian-Beaufort	Eocene	38	0.31	0.55	0.61	0.59	1.10
S4	Canadian-Beaufort	Early Eocene	26	0.48	0.49	0.45	0.26	1.08
S5	North Slope, Alaska	Mid-Late Eocene	32	0.24	0.41	0.26	0.08	0.77
S6	North Slope, Alaska	Mid-Late Eocene	32	0.24	0.40	0.28	0.07	0.97
S7	Canadian-Beaufort	Early Eocene	34	0.41	0.56	0.41	0.22	0.91
S8	Indonesia	Late Eocene	30	n.d.[d]	n.d.[d]	n.d.[d]	n.d.[d]	n.d.[d]
S9	Brunei	Mid-Miocene	87	0.06	0.25	0.31	n.d.[d]	0.83
S10	Brunei	Mid-Miocene	57	0.00	0.07	0.33	n.d.[d]	6.11

[a] C_{29} sterane percentage (in C_{27} – C_{29}) determined using GC-MRM-MS transition $M^+ \rightarrow 217$
[b] ratio determined from areas of GC-MRM-MS transitions $M^+ \rightarrow 217$ for C_{27} to C_{29} steranes
[c] based on areas of the GC-MRM-MS transition mass to charge m/z 440 → 191
[d] biomarkers were absent in this sample
[e] calculated from the 20*S* and 20*R* C_{29} sterane areas of transition parent ion → 217
[f] calculated from the $\alpha\alpha\alpha$-C_{29} sterane areas of transition parent ion → 217

Table 3. Comparison of biomarker analysis of GC-MS, GC-MRM-MS, GCxGC-FID and GCxGC-TOFMS. UCM = unresolved complex mixture. All abbreviations are used as define in the text. $^{1}t_{R}$ = first dimension retention time.

biomarker classes	GC-MS	GC-MRM-MS	GCxGC-FID	GCxGC-TOFMS	Figure
maturity parameters	robust for most parameters limited by co-elution (steranes) and sensitivity	robust limited by co-elution e.g. steranes and bicadinanes	superior, values comparable to 1D GC resolves co-elution,e.g. steranes hopanoids and bicadinanes	superior, values comparable to 1D GC resolves co-elution, e.g. steranes hopanoids and bicadinanes	5
hydrocarbon fraction analysed	branched and cyclic hydrocarbons	branched and cyclic hydrocarbons	whole crude oil/rock extract	whole crude oil/rock extract	
hopanoids	several co-elution problems between series of hopanoids	resolves co-elution, involves detection of numerous transitions	complete resolution of all series of hopanoids in 1st and 2nd dimension	complete resolution of all series of hopanoids in 1st and 2nd dimension	6
steranes	strong co-elution	resolves co-elutions, involves detection of numerous transitions	complete resolution of steranes and diasteranes in 2nd dimension	complete resolution of steranes and diasteranes in 2nd dimension	6
	strong co-elution	interference of steranes and bicadinanes not resolved	complete resolution of steranes and bicadinanes	complete resolution of steranes and bicadinanes	6
co-elution with hopane	not detected	not detected	indication *via* peak shape	reveals co-elution of minor compounds with hopane	7

higher plant des-A-triterpenoids	GC-MS	GC-MRM-MS	GCxGC-FID	GCxGC-TOFMS	Figure
separation of: des-A-OI, des-A-L, des-A-U/T, compound 5 and compound 6	Yes	Yes	Yes	Yes	8
positive characterisation of des-A-U/T	No	No	Yes	Yes	-
separation of nor-des-A-U/T and des-A-L	No	Yes, no mass spectra for identification	Yes, no mass spectra	separation and identification	9a
detection and separation of des-A-lup-ene and peak 7	No	No	Yes	Yes	9b
detection and separation of des-A-lup-diene and peak 8	No	No	Yes	Yes	9b
visual groupings of saturated and mono-, di- and triaromatic des-A-compounds	No	No	Yes, if ^1t_R and ^2t_R known	Yes	9c
pentacyclic triterpenoids					
baseline separation of 18α(H)-, 18β(H)-oleanane and lupane	No	No	Yes	Yes	1, 3
separation of β-BNL and BNH	No	No	Yes, if ^1t_R and ^2t_R known	Yes	10
detection and separation of additional peaks near BNH	No	No	No	Yes	10
separation of 24-NL and 30-NH	No	No	Yes, if ^1t_R and ^2t_R known	Yes	10
separation of BNU/T and NH	No	No	Yes, if ^1t_R and ^2t_R known	Yes	10
separation of unsaturated pentacyclics	limited	limited	Yes, if ^1t_R and ^2t_R known	Yes	

(Table 3 continued)

7 Figure Captions

Fig. 1. GC-MS chromatograms of the saturated hydrocarbon fractions from selected oils and rock extracts. Pr = pristane, 24-NL = 24-norlupane (**XXIV**), nC$_{33}$ = n-alkane, Ph = phytane, iP = isopimarane (**V**), U = unidentified ring A-degraded compound, enes = mono- and di-unsaturated pentacyclics.

Fig. 2. Mountain plots of GC×GC-FID chromatograms for selected whole oils. (a) oil A1, the insert shows A1 in a different perspective emphasising the n-alkane distribution; (b) oil A2; (c) oil A3; (d) oil C3; (e) oil C4; (f) oil M1. ^1t_R and ^2t_R are given in seconds. Abundances are colour coded (blue = baseline, colour change from green to red with increasing abundance) and relative to the most abundant peak in each chromatogram. H = hopanes, S = steranes, N = naphthalenes, 25NH = 25-norhopanes, T = pentacyclic triterpenoids, B = benzenes.

Fig. 3. 3D GC×GC-FID chromatograms of selected rock extracts. (a) S1; (b) S3; (c) S6; (d) S9. Highlighted are characteristic areas in the chromatogram of each sample. Colour code as in Fig. 2.

Fig. 4. Comparison of the resolution of unresolved complex mixture (UCM) using (a) GC-MS, (b) GC-MRM-MS and (c) GC×GC-FID.

Fig. 5. C$_{32}$ homohopane isomerisation ratio 22S/(22S+22R) determined from GC-MS, GC-MRM-MS, GC×GC-FID and GC×GC-TOFMS. GC-MS, GC-MRM-MS and GC×GC-TOFMS provided ratios based on areas of the base ion (GC-MS and GC×GC-TOFMS, m/z 191), or one transition (GC-MRM-MS, m/z 440 → 191). The isomerisation ratios derived from GC×GC-FID were calculated from the total peak area. See Table 1 for sample identification.

Fig. 6. . Separation of hopanes (yellow) and steranes (Volkman et al.) using GC×GC-TOF in rock extract S7. Shown is the combined EIC of the masses *m/z* 191, 177, 205, 163, 190, 217 and 218. Key: H = hopane, 25 = 25-norhopane, HH = homohopane, NH = norhopane, BNH = bisnorhopane.

Fig. 7. Detected compounds partially co-eluting with C_{30}-hopane. (a) Section of the combined EIC of *m/z* 177, 355, 369 of rock extract S5. (b) section of the GC×GC-TOFMS total ion chromatogram (TIC) of S5 (c) – (f) mass spectra of compounds 1 – 4.

Fig. 8. . Elution order and mass spectra of tetracyclic terpenoids. GC×GC-TOFMS chromatograms of *m/z* 330 + 191 of (a) oil C2, and (b) S7. The elution pattern is a straight line across the first and second dimension. The peak abundance is colour coded with increasing abundance from green to red. (c) - (f) show GC×GC-TOFMS mass spectra of des-A-oleanane (**XV**), des-A-ursane/taraxastane (**XVII**), compound 5 and compound 6. Des-A-Ol = des-A-oleanane (**XV**), des-A-L = des-A-lupane (**XVI**), des-E-H = des-E- hopane (**XVIII**). Des-A-compounds were positively identified via comparison of GC-MS, GC-MRM-MS and GCxGC-TOF chromatograms and mass spectra with elution orders and mass spectra reported in the literature which is discussed in the text.

Fig. 9. GC×GC-TOFMS ion chromatograms illustrating elution order and separation results for tetracyclic triterpenoids in oil C2. (a) extracted ion chromatogram *m/z* 330 + 316; (b) extracted ion chromatogram *m/z* 328 + 326; (c) extracted ion chromatogram *m/z* 330 + 310 + 292 + 274 representing saturated, mono-, di- and triaromatic tetracyclic triterpenoids. O = oleanane (**I**), U/T = ursane/taraxastanes, L = lupane (**II**), H = hopane. Dashed lines represent the location of the series. Des-A-compounds were tentatively identified via comparison of GC-MS, GC-MRM-MS and GCxGC-TOF chromatograms and mass spectra with elution orders and mass spectra reported in the literature.

Fig. 10. Section of the combined GC×GC-TOFMS EIC of the masses *m/z* 191, 177, 205, 412, 410, 398, 396, 384, 218 of rock extract S1. Key: dashed

circles indicate groups of compounds (especially unidentified compounds based on the same molecular mass. Red: M^+ = 384, orange: M^+ = 398, black: M^+ = 410. ß-Tm = 22,29,30-trinor-17ß-hopane, α-BNL = 17α-24,28-bisnorlupane (**XXVII**), ß-BNL = 17ß-24,28-bisnorlupane (**XXIII**), BNH = 28,30-bisnorhopane, BNO = tentatively identified as 24,28-bisnoroleanane (**XXV**), NH = 30-norhopane, BNU/T – tentatively identified as 24,28-bisnorursane/taraxastane (**XXVI**), 24NL = 24-norlupane (**XXIV**), NM = 30-normoretane, H = 17α,21ß(H)-hopane, α-O = 18α(H)-oleanane (**I**), ß-O = 18ß(H)-oleanane (**II**), L = lupane (**III**), ßß-NH = 17ß,21ß(H)-30-norhopane, M = moretane. Compounds not described in the methods and materials were tentatively identified via comparison of GC-MS, GC-MRM-MS and GCxGC-TOF chromatograms and mass spectra with elution orders and mass spectra reported in the literature.

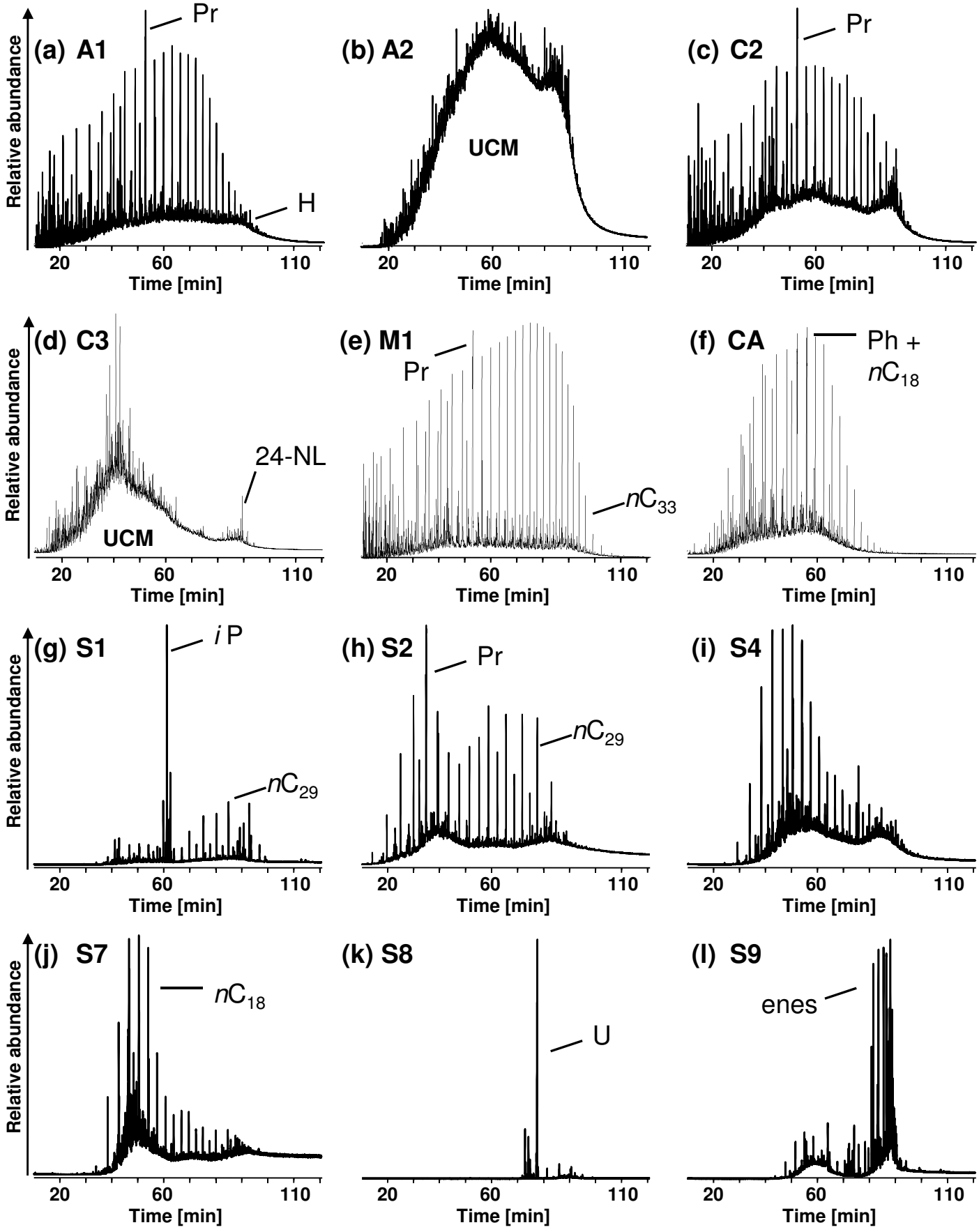
(a) A1
Pr
H
(b) A2
UCM
(c) C2
Pr
(d) C3
24-NL
UCM
(e) M1
Pr
nC33
(f) CA
Ph +
nC18
(g) S1
i P
nC29
(h) S2
Pr
nC29
(i) S4
(j) S7
nC18
(k) S8
U
(l) S9
enes
Relative abundance
Time [min]
20
60
110

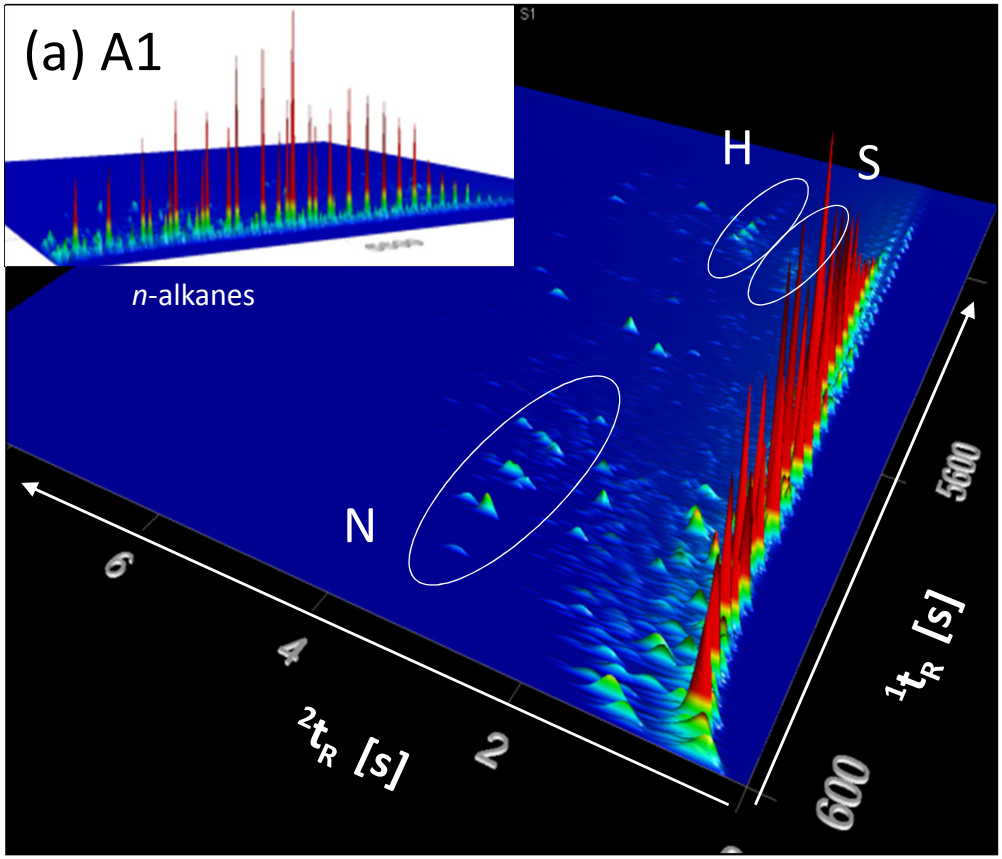
(a) A1
S1
n-alkanes
H
S
N
6
4
2
2tR [s]
600
5600
1tR [s]

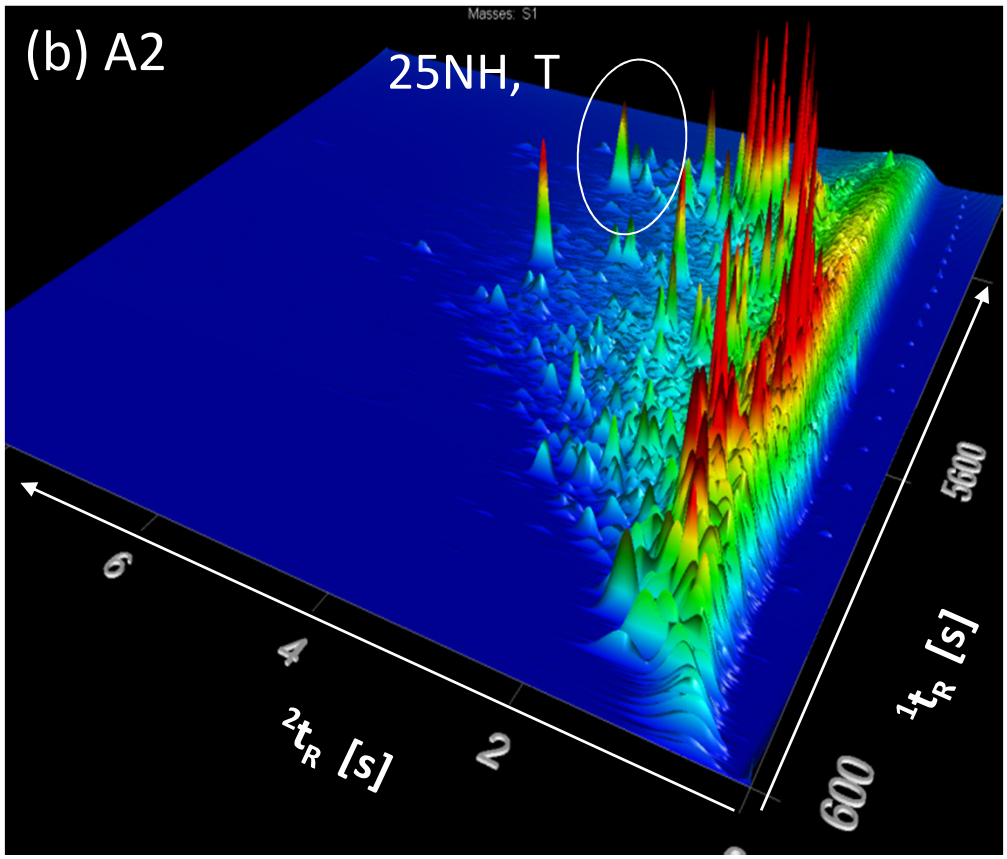
(b) A2
Masses: S1
25NH, T
6
4
2
2tR [s]
600
5600
1tR [s]

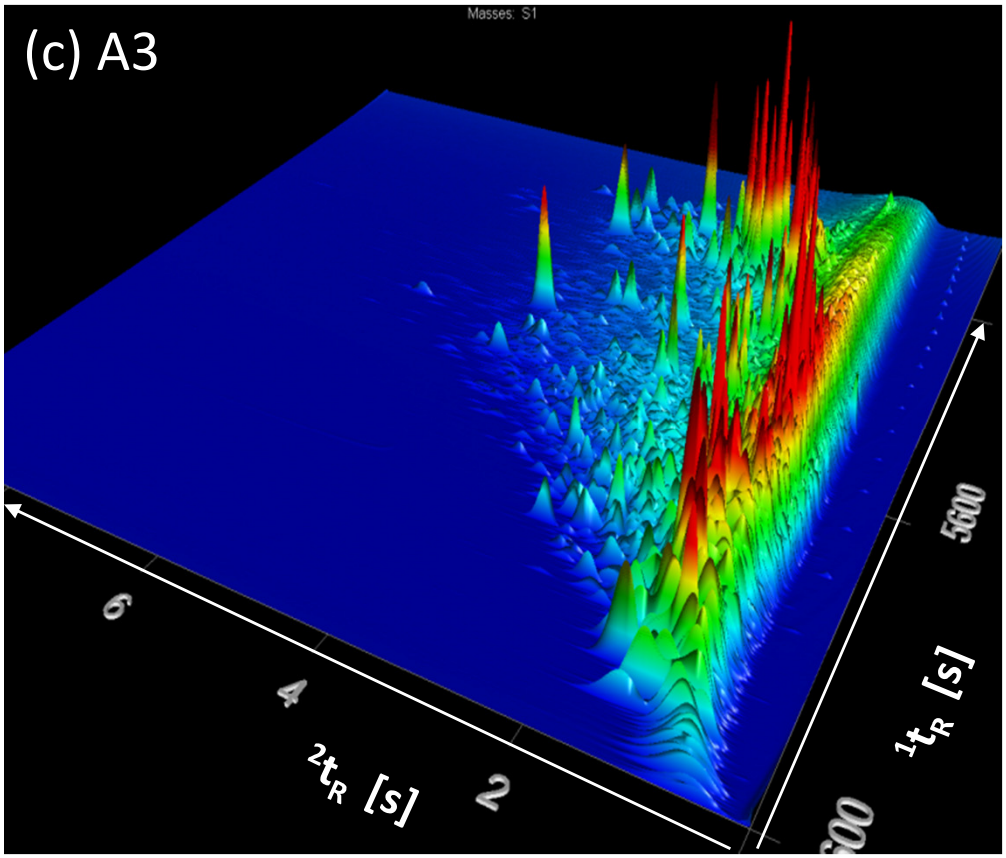
Masses: S1
(c) A3
6
4
^2t_R [s]
2
^1t_R [s]
600

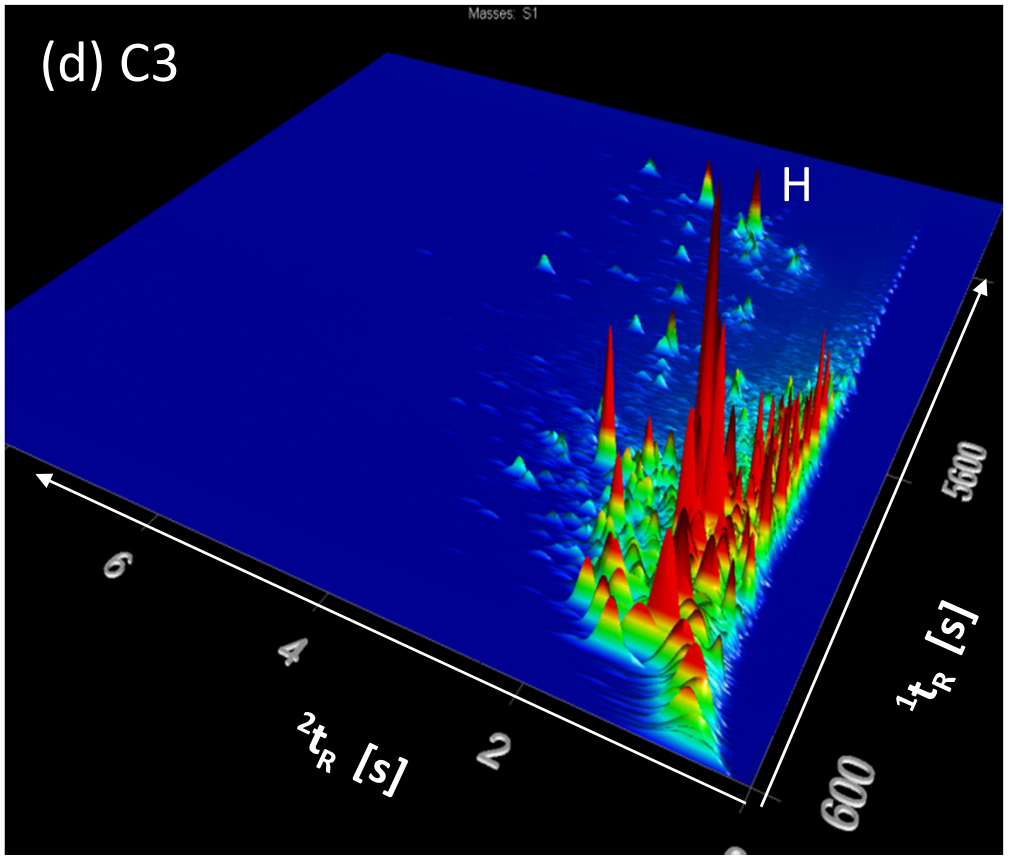
Masses: S1
(d) C3
H
6
4
^2t_R [s]
2
600
^1t_R [s]

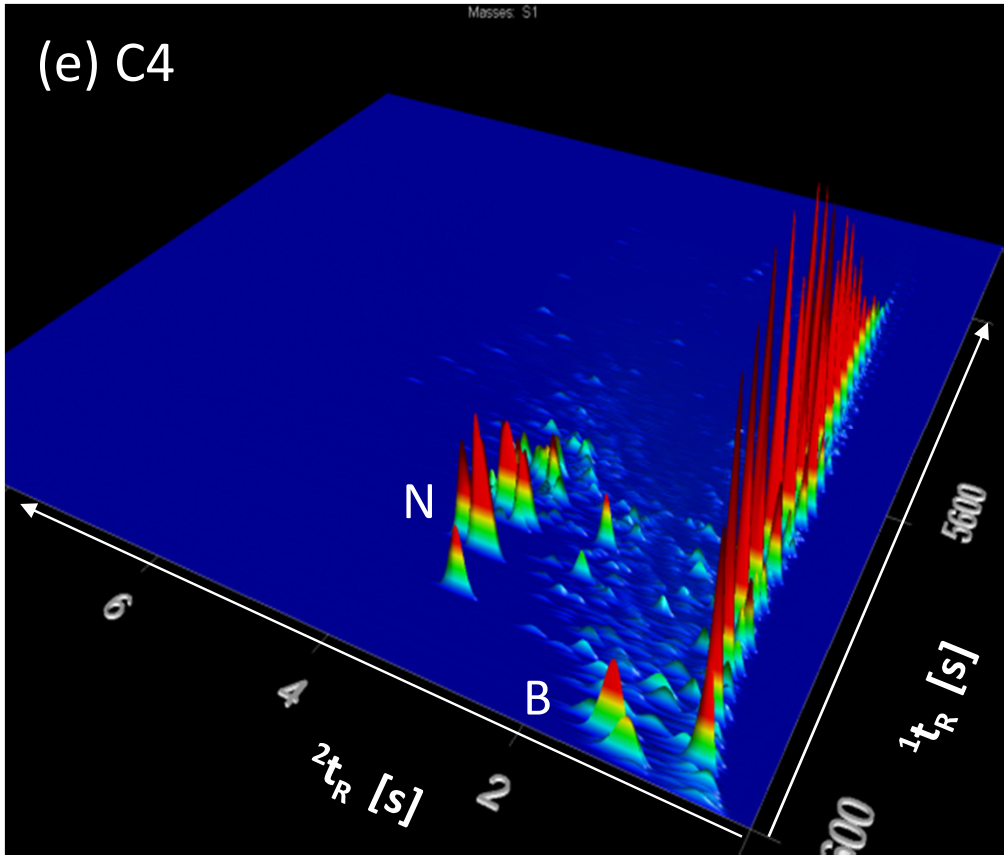
Masses: S1
(e) C4
N
B
6
4
2
^2t_R [s]
5600
^1t_R [s]

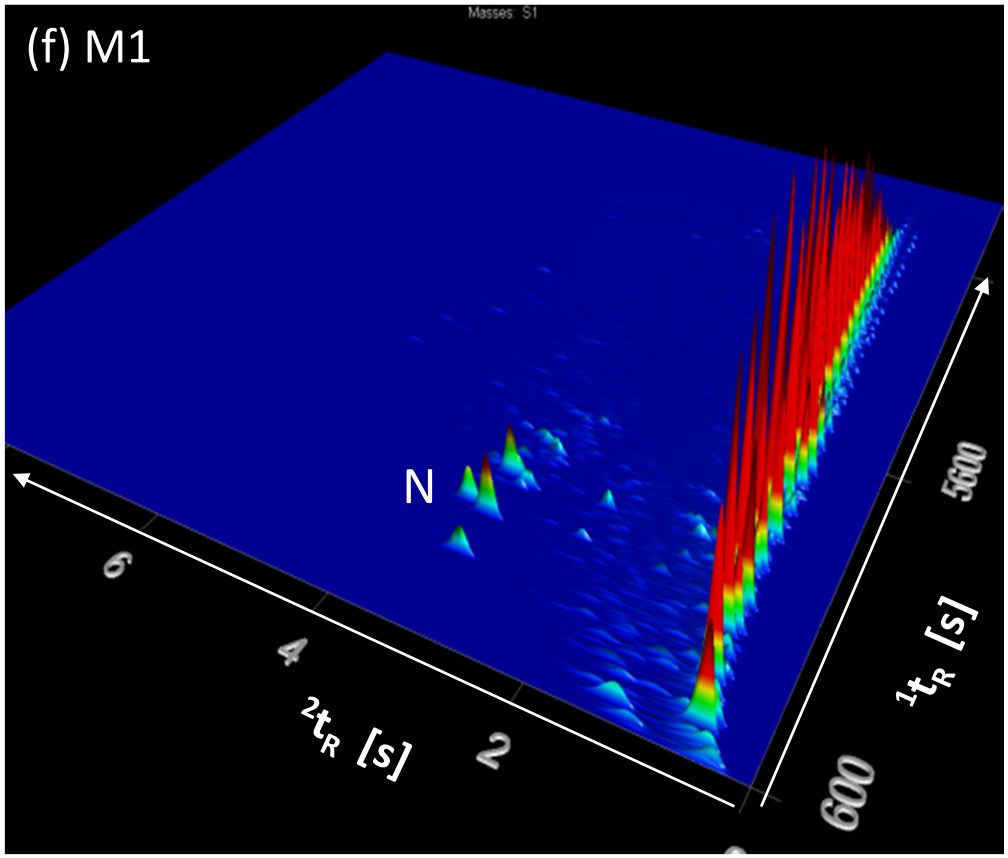
Masses: S1
(f) M1
N
6
4
2
^2t_R [s]
600
5600
^1t_R [s]

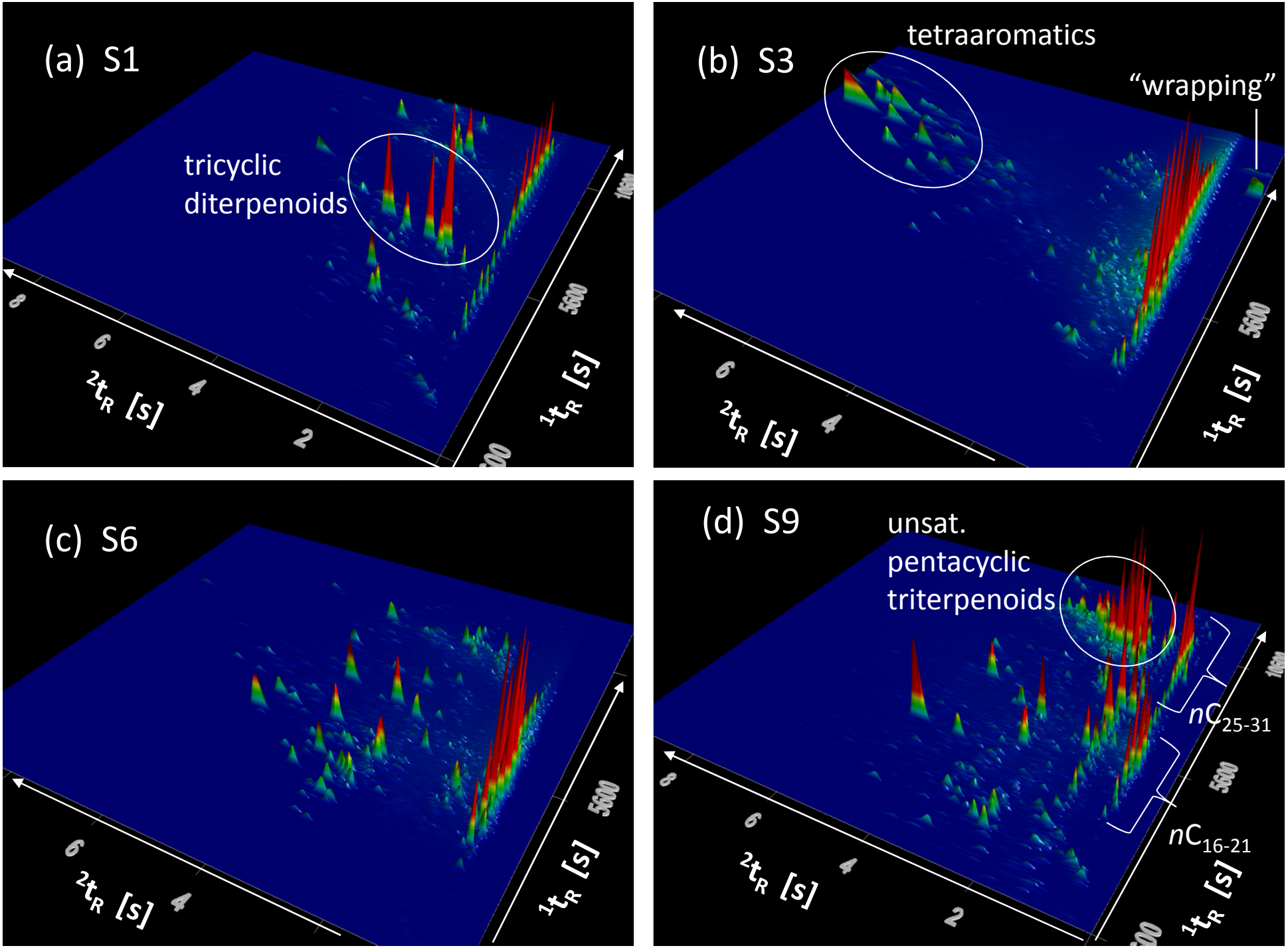
(a) S1
tricyclic
diterpenoids
(b) S3
tetraaromatics
"wrapping"
(c) S6
(d) S9
unsat.
pentacyclic
triterpenoids
nC25-31
nC16-21
2tR [s]
1tR [s]

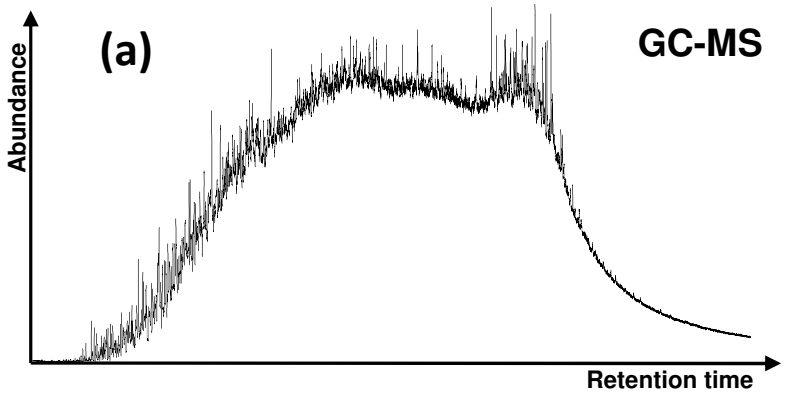
(a)
GC-MS
Abundance
Retention time

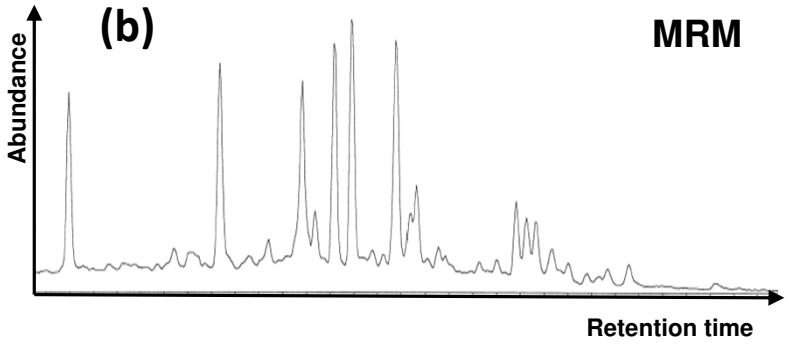
(b)
MRM
Abundance
Retention time

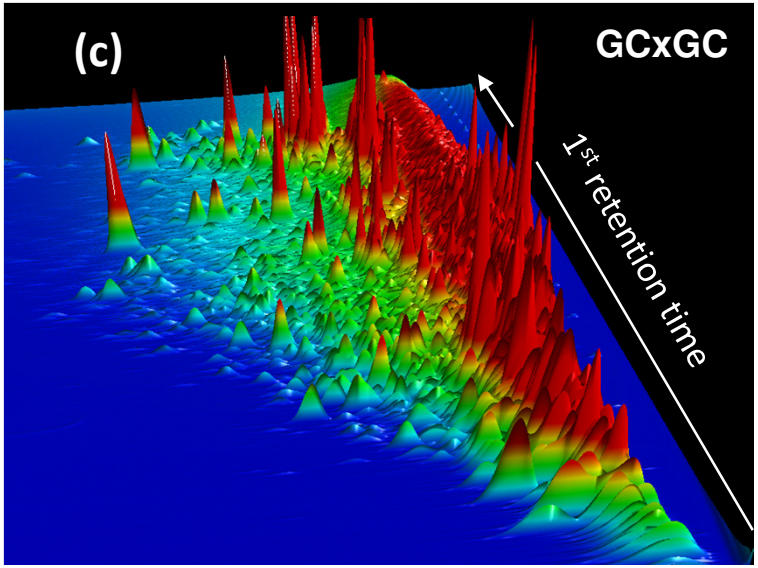
(c)
GCxGC
1st retention time

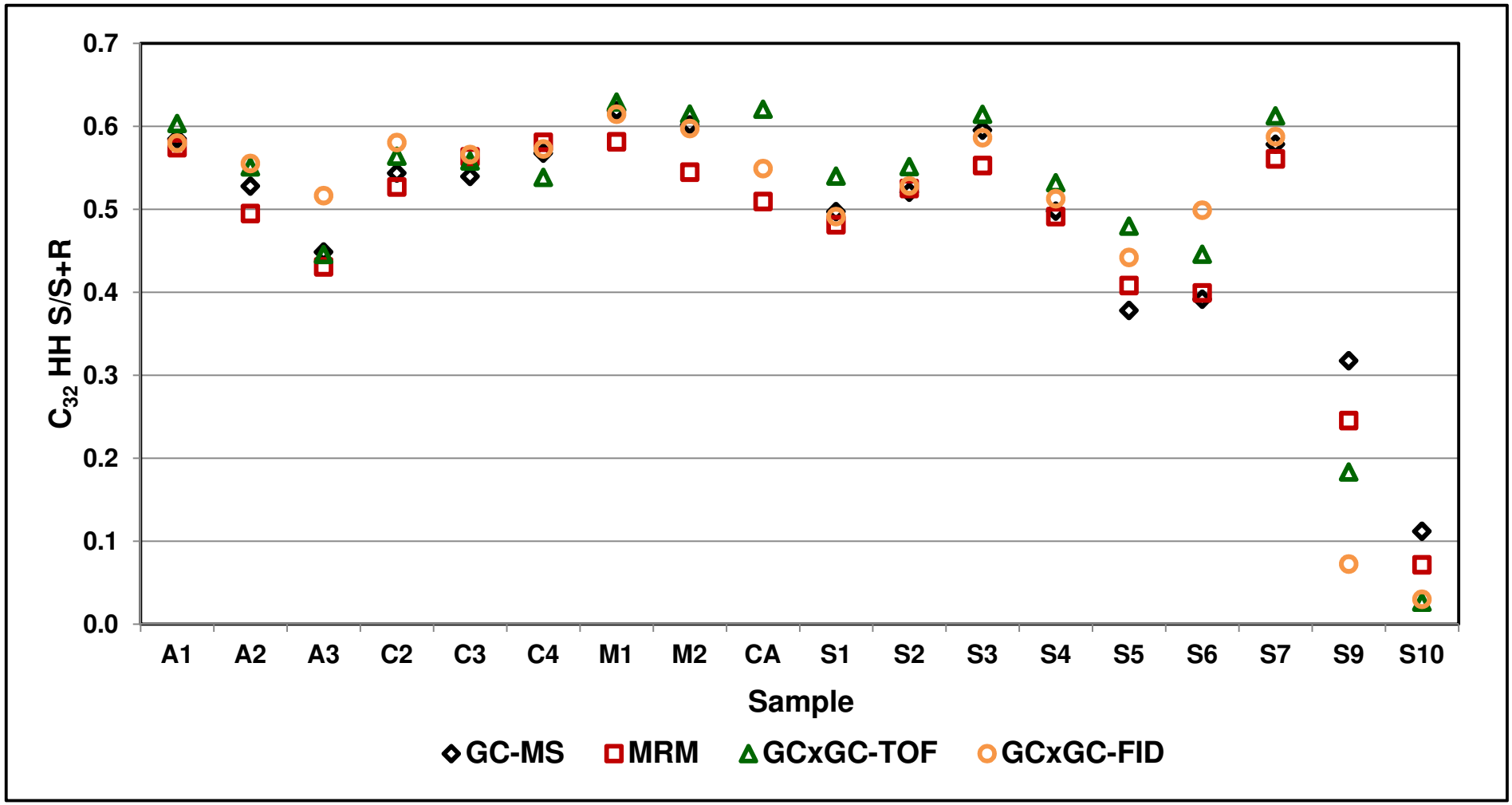
0.7
0.6
0.5
0.4
0.3
0.2
0.1
0.0
C32 HH S/S+R
A1
A2
A3
C2
C3
C4
M1
M2
CA
S1
S2
S3
S4
S5
S6
S7
S9
S10
Sample
GC-MS
MRM
GCxGC-TOF
GCxGC-FID

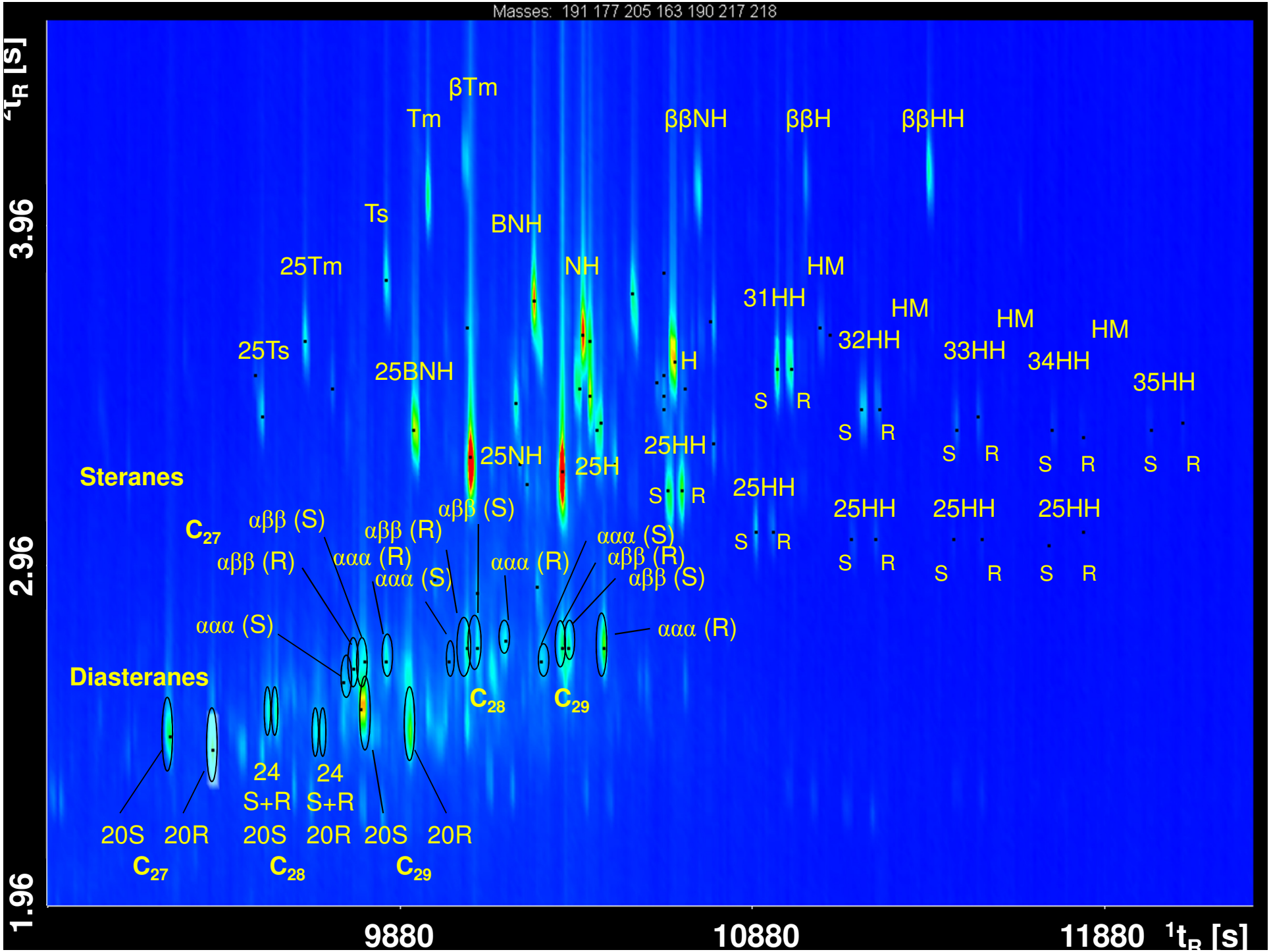
Masses: 191 177 205 163 190 217 218
^2t_R [s]
3.96
2.96
1.96
9880
10880
11880
^1t_R [s]
βTm
Tm
βββNH
ββH
ββHH
Ts
BNH
25Tm
NH
HM
31HH
HM
HM
HM
32HH
33HH
34HH
35HH
25Ts
25BNH
H
S R
S R
S R
S R
S R
25NH
25H
25HH
Steranes
S R
25HH
25HH
25HH
25HH
αββ (S)
αββ (R)
αββ (R)
αββ (S)
C27
ααα (S)
ααα (R)
ααα (S)
ααα (R)
αββ (R)
αββ (S)
ααα (S)
ααα (R)
Diasteranes
C28
C29
24
S+R
24
S+R
20S
20R
20S
20R
20S
20R
C27
C28
C29

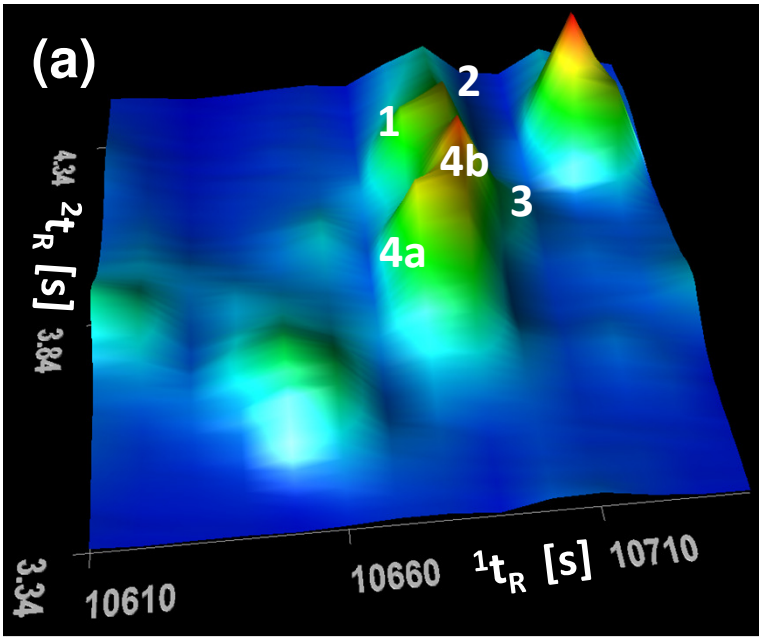
(a)
1
2
4b
3
4a
4.34
2tR [s]
3.84
3.34
10610
10660
1tR [s]
10710

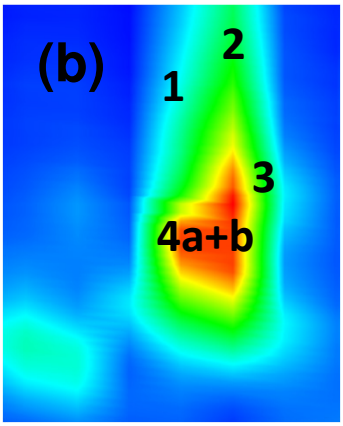
(b)
1
2
3
4a+b

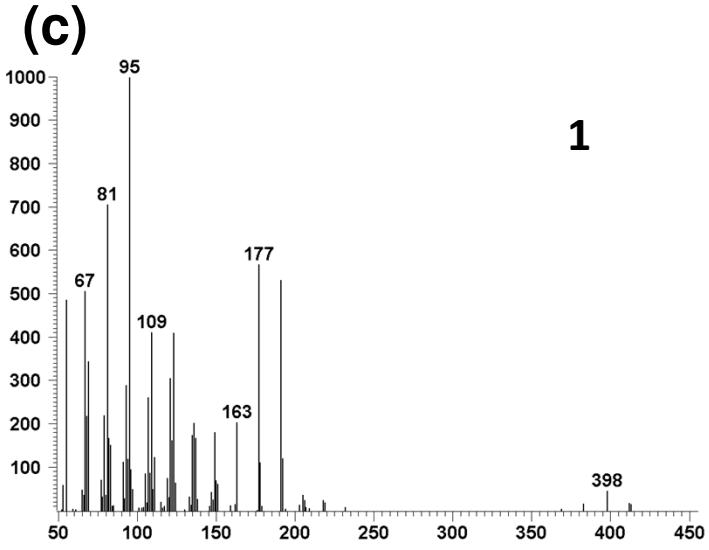
(c)
1
95
81
67
109
177
163
398

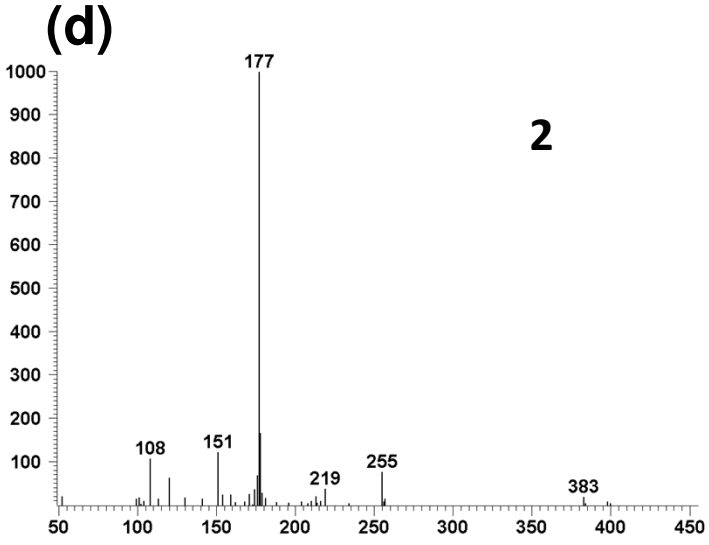
(d)
2
177
108
151
219
255
383

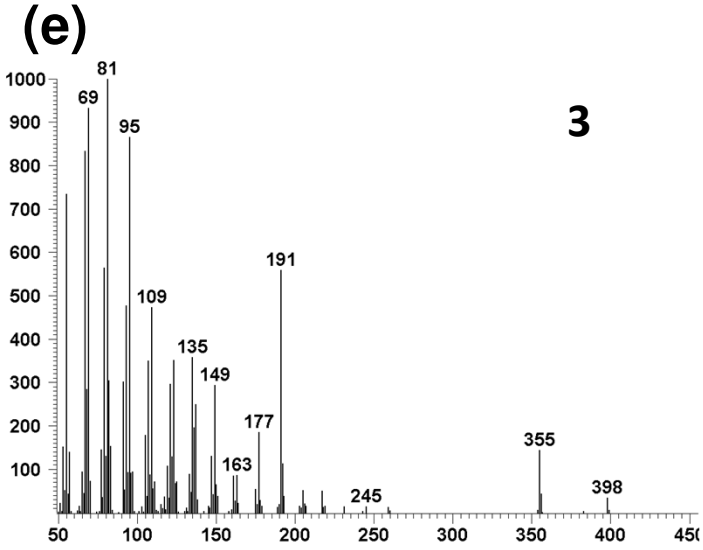
(e)
3
81
69
95
191
109
135
149
177
163
355
245
398

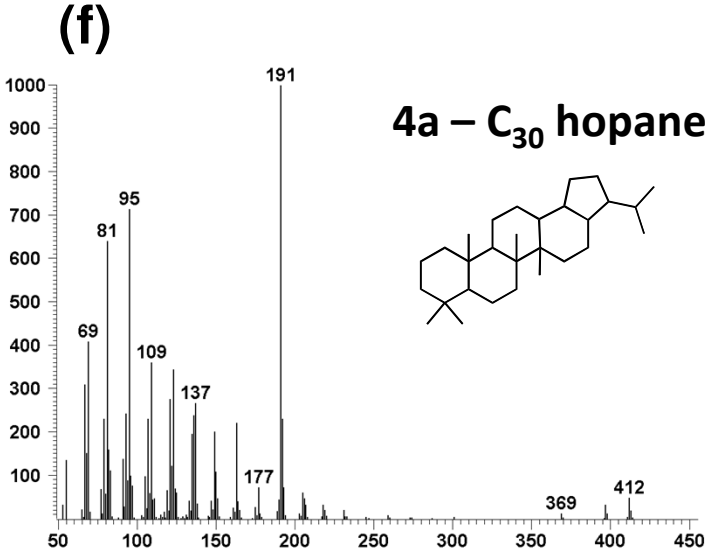
(f)
4a – C30 hopane
191
95
81
69
109
137
177
369
412

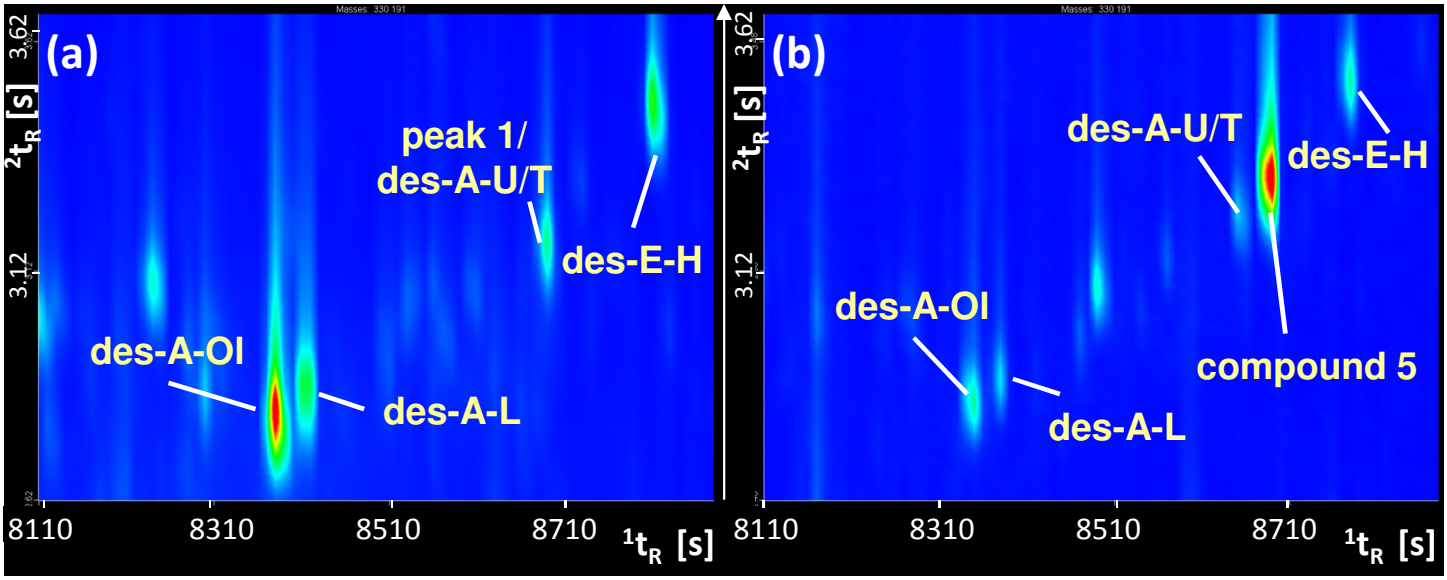
(a)
peak 1/
des-A-U/T
des-E-H
des-A-Ol
des-A-L
(b)
des-A-U/T
des-E-H
des-A-Ol
compound 5
des-A-L
3.62
3.12
2tR [s]
8110
8310
8510
8710
1tR [s]

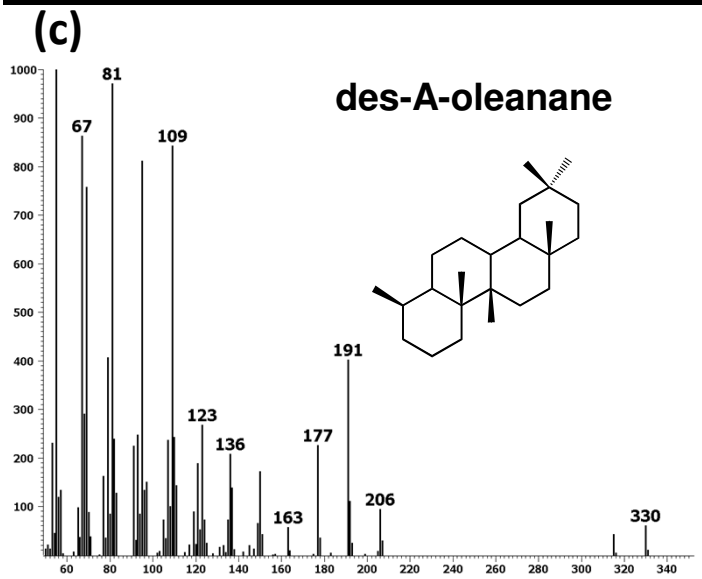
(c)
des-A-oleanane
81
67
109
191
123
136
177
163
206
330

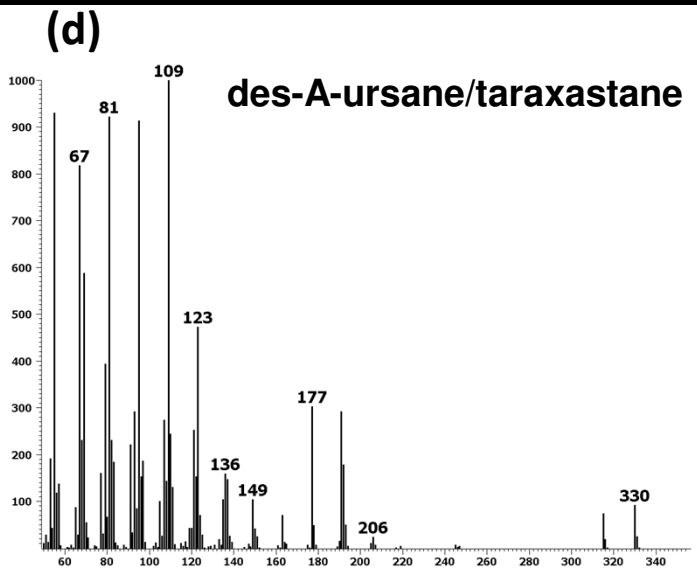
(d)
des-A-ursane/taraxastane
109
81
67
123
177
136
149
206
330

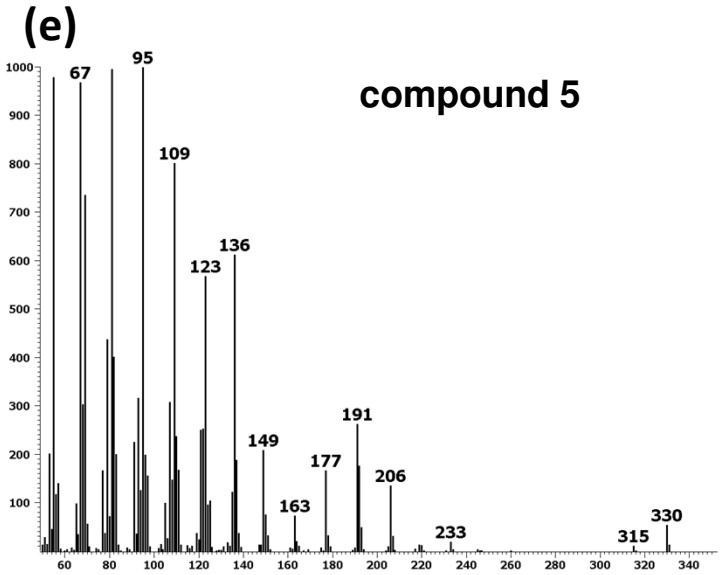
(e)
compound 5
95
67
109
136
123
149
191
177
163
206
233
315
330

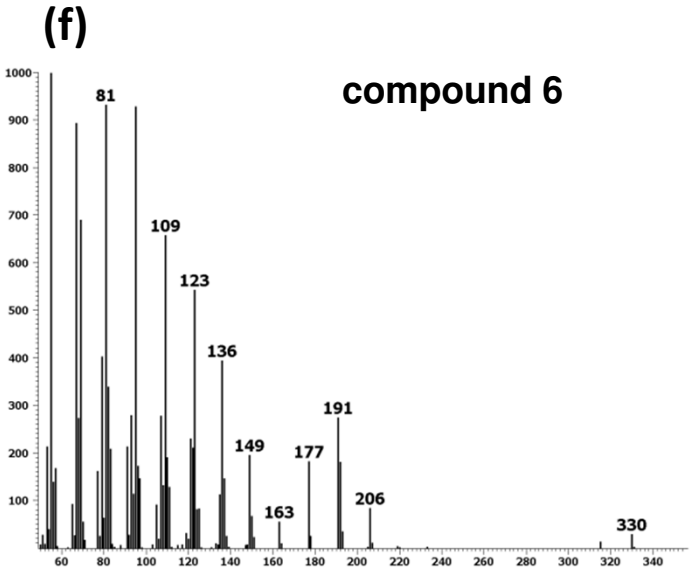
(f)
compound 6
81
109
123
136
191
149
177
163
206
330

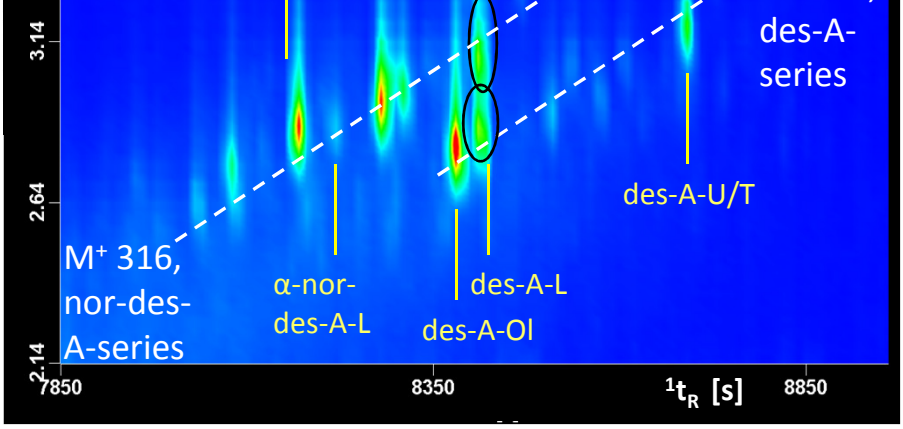
des-A-
series
des-A-U/T
M+ 316,
nor-des-
A-series
α-nor-
des-A-L
des-A-L
des-A-OI
3.14
2.64
2.14
7850
8350
1tR [s]
8850

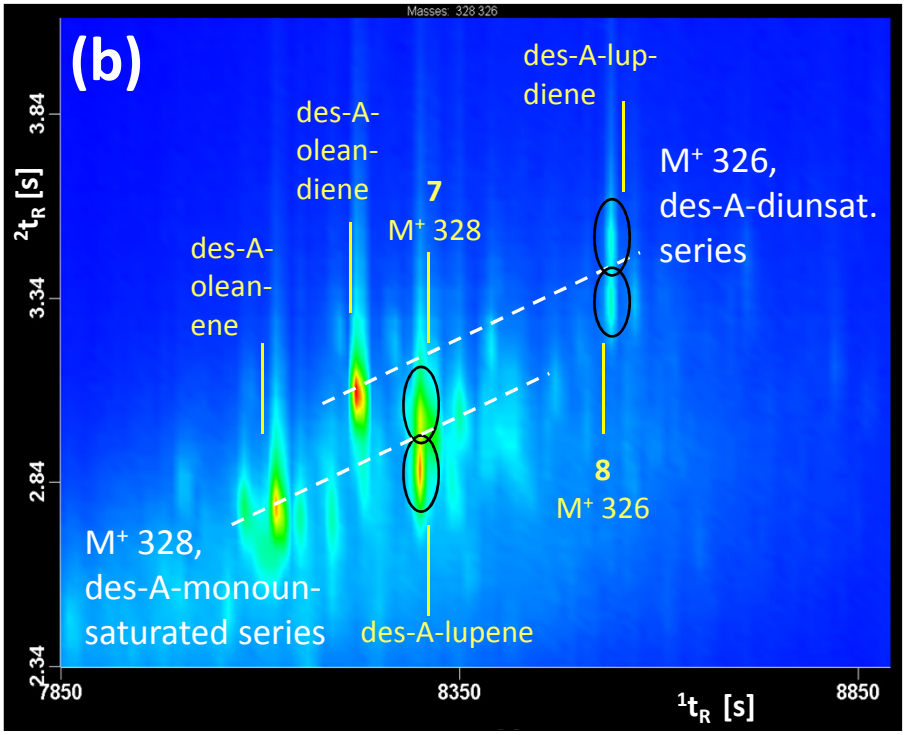
Masses: 328 326
(b)
des-A-lup-
diene
des-A-
olean-
diene
7
M+ 328
M+ 326,
des-A-diunsat.
series
des-A-
olean-
ene
8
M+ 326
M+ 328,
des-A-monoun-
saturated series
des-A-lupene
3.84
3.34
2.84
2.34
2tR [s]
7850
8350
1tR [s]
8850

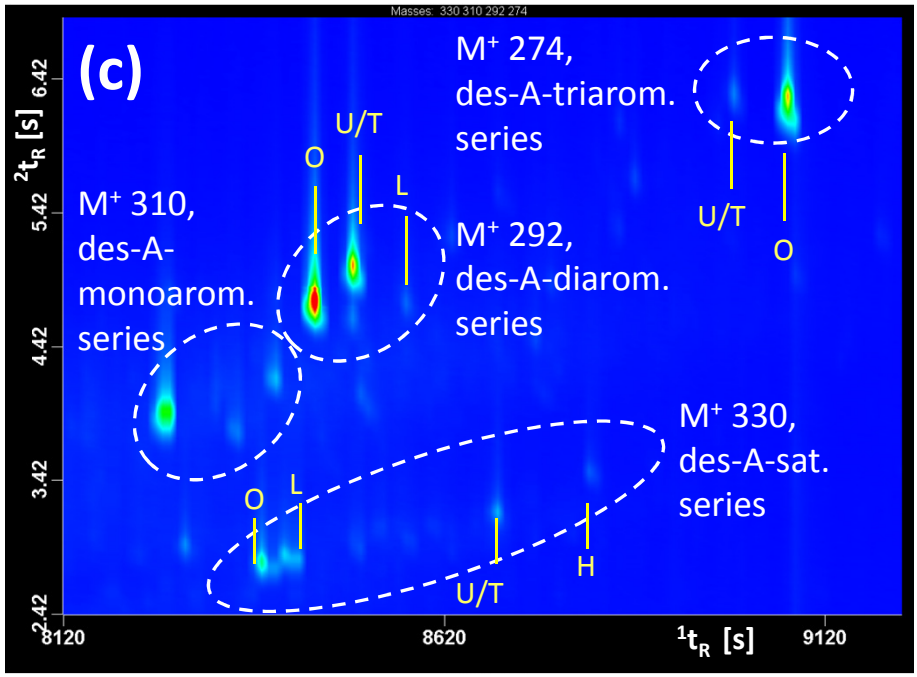
Masses: 330 310 292 274
(c)
M+ 274,
des-A-triarom.
series
U/T
O
L
M+ 310,
des-A-
monoarom.
series
M+ 292,
des-A-diarom.
series
U/T
O
M+ 330,
des-A-sat.
series
O
L
H
U/T
6.42
5.42
4.42
3.42
2.42
2tR [s]
8120
8620
1tR [s]
9120

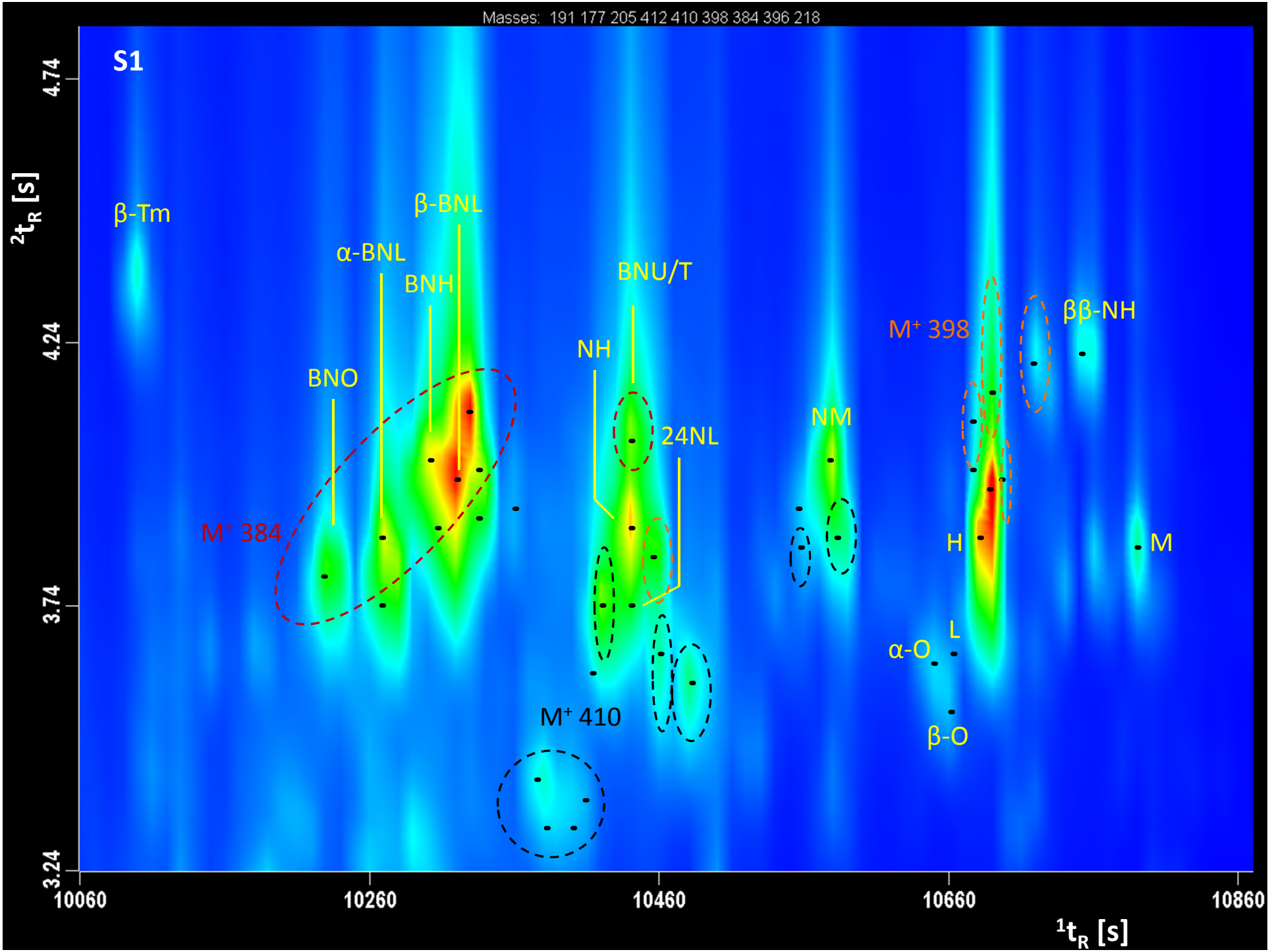
Masses: 191 177 205 412 410 398 384 396 218
S1
β-Tm
β-BNL
α-BNL
BNH
BNO
BNU/T
NH
24NL
NM
M+ 398
ββ-NH
M+ 384
M+ 410
H
M
L
α-O
β-O
4.74
4.24
3.74
3.24
2tR [s]
10060
10260
10460
10660
10860
1tR [s]